Geobiology (2007), **5**, 169–189 DOI: 10.1111/j.1472-4669.2007.00103.x

The mechanisms of iron isotope fractionation produced during dissimilatory Fe(III) reduction by *Shewanella putrefaciens* and *Geobacter sulfurreducens*

HEIDI A. CROSBY, ERIC E. RODEN, CLARK M. JOHNSON AND BRIAN L. BEARD

Department of Geology and Geophysics, University of Wisconsin-Madison, Madison, WI 53706, USA

ABSTRACT

Microbial dissimilatory iron reduction (DIR) is widespread in anaerobic sediments and is a key producer of aqueous Fe(II) in suboxic sediments that contain reactive ferric oxides. Previous studies have shown that DIR produces some of the largest natural fractionations of stable Fe isotopes, although the mechanism of this isotopic fractionation is not yet well understood. Here we compare Fe isotope fractionations produced by similar cultures of *Geobacter sulfurreducens* strain PCA and *Shewanella putrefaciens* strain CN32 during reduction of hematite and goethite. Both species produce aqueous Fe(II) that is depleted in the heavy Fe isotopes, as expressed by a decrease in $^{56}Fe/^{54}Fe$ ratios or $\delta^{56}Fe$ values. The low $\delta^{56}Fe$ values for aqueous Fe(II) produced by DIR reflect isotopic exchange among three Fe inventories: aqueous Fe(II) ($Fe(II)_{aq}$), sorbed Fe(II) ($Fe(II)_{sorb}$), and a reactive Fe(III) component on the ferric oxide surface ($Fe(III)_{reac}$). The fractionation in $^{56}Fe/^{54}Fe$ ratios between $Fe(II)_{aq}$ and $Fe(III)_{reac}$ was –2.95‰, and this remained constant over the timescales of the experiments (280 d). The $Fe(II)_{aq}$ – $Fe(III)_{reac}$ fractionation was independent of the ferric Fe substrate (hematite or goethite) and bacterial species, indicating a common mechanism for Fe isotope fractionation during DIR. Moreover, the $Fe(II)_{aq}$ – $Fe(III)_{reac}$ fractionation in $^{56}Fe/^{54}Fe$ ratios during DIR is identical within error of the equilibrium $Fe(II)_{aq}$ – ferric oxide fractionation in abiological systems at room temperatures. This suggests that the role of bacteria in producing Fe isotope fractionations during DIR lies in catalyzing coupled atom and electron exchange between $Fe(II)_{aq}$ and $Fe(III)_{reac}$ so that equilibrium Fe isotope partitioning occurs.

Although Fe isotope fractionation between $Fe(II)_{aq}$ and $Fe(III)_{reac}$ remained constant, the absolute $\delta^{56}Fe$ values for $Fe(II)_{aq}$ varied as a function of the relative proportions of $Fe(II)_{aq}$, $Fe(II)_{sorb}$, and $Fe(III)_{reac}$ during reduction. The temporal variations in these proportions were unique to hematite or goethite but independent of bacterial species. In the case of hematite reduction, the small measured $Fe(II)_{aq}$ – $Fe(II)_{sorb}$ fractionation of –0.30‰ in $^{56}Fe/^{54}Fe$ ratios, combined with the small proportion of $Fe(II)_{sorb}$, produced insignificant (<0.05‰) isotopic effects due to sorption of Fe(II). Sorption of Fe(II) produced small, but significant effects during reduction of goethite, reflecting the higher proportion of $Fe(II)_{sorb}$ and larger measured $Fe(II)_{aq}$ – $Fe(II)_{sorb}$ fractionation of –0.87‰ in $^{56}Fe/^{54}Fe$ ratios for goethite. The isotopic effects of sorption on the $\delta^{56}Fe$ values for $Fe(II)_{aq}$ were largest during the initial stages of reduction when $Fe(II)_{sorb}$ was the major ferrous Fe species during goethite reduction, on the order of 0.3 to 0.4‰. With continued reduction, however, the isotopic effects of sorption decreased to <0.2‰. These results provide insight into the mechanisms that produce Fe isotope fractionation during DIR, and form the basis for interpretation of Fe isotope variations in modern and ancient natural systems where DIR may have driven Fe cycling.

Received 12 November 2006; accepted 07 February, 2007

Corresponding author: E. E. Roden, Tel.: 608-890-0727; fax: 608-262-0693; e-mail: eroden@geology.wisc.edu.

INTRODUCTION

Dissimilatory iron-reducing bacteria are unique in their ability to generate energy by coupling oxidation of organic matter and H_2 to reduction of solid ferric oxides and hydroxides (Lovley *et al.*, 2004). Dissimilatory iron reduction (DIR) is a widespread process in anaerobic sediments (Thamdrup, 2000), and may be one of the oldest forms of respiration (Vargas *et al.*, 1998). DIR is an important source of aqueous Fe(II), which readily adsorbs to oxide surfaces and catalyses the

reduction of a number of organic and inorganic contaminants (Buerge & Hug, 1999; Liger *et al.*, 1999; Amonette *et al.*, 2000; Pecher *et al.*, 2002; Strathmann & Stone, 2003; Elsner *et al.*, 2004; Fredrickson *et al.*, 2004; Williams *et al.*, 2005).

Previous laboratory experiments have investigated Fe isotope fractionations during DIR, and all have found that aqueous Fe(II) ($Fe(II)_{aq}$) that is produced is depleted in the heavy Fe isotopes. The $^{56}Fe/^{54}Fe$ ratios of $Fe(II)_{aq}$ are ~0.1–0.25% (1–2.5‰) lower than the initial ferric oxide or hydroxide substrate, and this has been taken as a 'biosignature' for DIR (Johnson *et al.*, 2005). Alternatively, it has been proposed that the low-$^{56}Fe/^{54}Fe$ 'signature' of $Fe(II)_{aq}$ produced by DIR may be due to sorption of Fe(II) ($Fe(II)_{sorb}$) and therefore unrelated to biology (Icopini *et al.*, 2004). Resolution of these contrasting interpretations requires a detailed mechanistic understanding of the Fe isotope fractionations produced during DIR, including the role of $Fe(II)_{sorb}$. Increasing our understanding of the mechanisms involved in Fe isotope fractionation is important, given the effort to find an Fe isotope fingerprint for DIR in modern and ancient sedimentary environments (Beard *et al.*, 1999; Matthews *et al.*, 2004; Yamaguchi *et al.*, 2005; Archer & Vance, 2006; Johnson & Beard, 2006; Severmann *et al.*, 2006; Staubwasser *et al.*, 2006).

The objective of this work was to compare Fe isotope fractionation produced during ferric oxide reduction by *Shewanella putrefaciens* to our earlier results obtained with *Geobacter sulfurreducens* (Crosby *et al.*, 2005). Although members of the Geobacteraceae require direct contact with the oxide surface for reduction to occur (Nevin & Lovley, 2000; Childers *et al.*, 2002), *Shewanella* species may be able to reduce Fe oxides indirectly by producing either electron-shuttling compounds or Fe chelators (Nevin & Lovley, 2002; Lies *et al.*, 2005). Recent studies have indicated that both *Geobacter* and *Shewanella* species are capable of synthesizing specialized electrically conductive pili ('nanowires'), which may provide a means for transporting electrons to insoluble Fe oxides (Reguera *et al.*, 2005; Gorby *et al.*, 2006). We find that when the two species are investigated under identical non-growth conditions, and where direct contact with Fe oxides (hematite and goethite) is allowed, the Fe isotope compositions of $Fe(II)_{aq}$ are largely controlled by the specific Fe oxide or hydroxide and independent of the bacterial species. In addition to calculating Fe isotope fractionations, we use the powerful constraints imposed by isotopic mass-balance to calculate the changing abundance of the various reactive Fe pools that are open to atom (isotopic) exchange during DIR, and show how these exert a fundamental control on the Fe isotope compositions of $Fe(II)_{aq}$ produced by DIR.

PREVIOUS WORK

Prior studies of Fe isotope fractionation produced during DIR include those of Beard *et al.* (1999, 2003a), Icopini *et al.* (2004), Johnson *et al.* (2005), and Crosby *et al.* (2005). It has been proposed that the decrease in $^{56}Fe/^{54}Fe$ ratios of $Fe(II)_{aq}$, relative to the initial Fe oxide or hydroxide, occurred through isotopic exchange with an organic-ligand-bound, high-$^{56}Fe/^{54}Fe$ Fe(III) component (Beard *et al.*, 2003a; Johnson *et al.*, 2004). With the exception of the work of Crosby *et al.* (2005), however, none of the previous studies directly measured the high-$^{56}Fe/^{54}Fe$ component that is required by isotopic mass balance. Crosby *et al.* (2005) determined that the high $^{56}Fe/^{54}Fe$ component was a reactive Fe(III) layer on the oxide surface, defined as $Fe(III)_{reac}$, which was sampled through successive acid extractions, indicating that the 'ligand fractionation model' of Beard *et al.* (2003a) and Johnson *et al.* (2004) is incorrect. Three isotopically distinct pools of Fe were identified during dissimilatory reduction of hematite and goethite by *Geobacter sulfurreducens*: $Fe(II)_{aq}$, $Fe(II)_{sorb}$, and $Fe(III)_{reac}$ (Crosby *et al.*, 2005). Because these pools undergo changes in their isotopic compositions relative to the initial hematite or goethite, they may be collectively considered a 'reactive Fe pool' that was open to atom exchange during DIR. The isotopic fractionations between $Fe(II)_{aq}$ and $Fe(III)_{reac}$ match those determined in equilibrium experiments (Skulan *et al.*, 2002; Welch *et al.*, 2003), and Crosby *et al.* (2005) interpreted this to reflect coupled electron and atom exchange between Fe(II) and the oxide surface (Fig. 1). Here we combine new results obtained on reduction of hematite and goethite by *S. putrefaciens* with previous identical experiments using *G. sulfurreducens* to develop a more comprehensive model for Fe isotope fractionation during DIR.

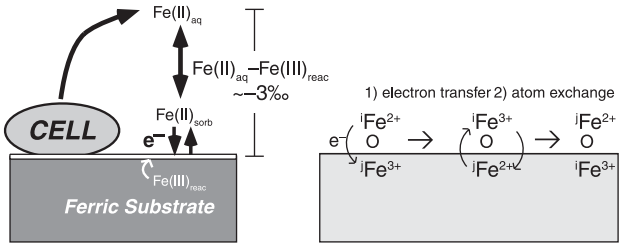

Fig. 1 Mechanism of Fe isotope fractionation during DIR through coupled atom and electron exchange (model based on Crosby *et al.*, 2005). The left side illustrates bacterial reduction of the ferric substrate, either hematite or goethite (not to scale). Some of the aqueous Fe(II) ($Fe(II)_{aq}$) produced sorbs to the oxide surface ($Fe(II)_{sorb}$), and then undergoes electron transfer and Fe(II)–Fe(III) atom exchange, producing a reactive layer of Fe(III) at the oxide surface ($Fe(III)_{reac}$) that has $^{56}Fe/^{54}Fe$ ratios which are higher than those of the initial substrate, balanced by $Fe(II)_{aq}$ that has $^{56}Fe/^{54}Fe$ ratios which are lower than the initial substrate. The overall isotopic fractionation between $Fe(II)_{aq}$ and ($Fe(III)_{reac}$) would be approximately –3‰ if it reflects equilibrium fractionation at room temperature. The right side of the figure provides an expanded view of the oxide surface, illustrating interactions between Fe atoms i and j at the oxide surface. In this model, sorbed Fe(II) (atom i) transfers an electron to an Fe(III) atom (j) of the oxide. In the second step, isotopic exchange of atoms i and j occurs, as required by the Fe isotope changes observed by Crosby *et al.* (2005).

MATERIALS AND METHODS

Fe(III) oxides

Hematite (α-Fe_2O_3) was purchased from Fisher Scientific (Naltham, MA, USA), and XRD and Mössbauer analyses indicated it was essentially pure. Particles were approximately spherical, with an average diameter of ~100 nm (Fig. 2) and a BET surface area of ~10 $m^2\ g^{-1}$. Medium surface area (MSA) goethite was synthesized by neutralization of ferric chloride (Schwertmann & Cornell, 1991), and again had no detectable impurities. Individual particles were elongated and had approximate dimensions of 30 × 160 nm (Fig. 2); the surface area measured by BET analysis was ~55 $m^2\ g^{-1}$. TEM images of the oxide materials before and after the experiment showed no obvious changes in particle morphology. Partial dissolution studies using weak HCl indicated that the hematite and goethite are isotopically homogenous (see below).

Bacterial strains and culturing

The dissimilatory Fe(III)-reducing species *Geobacter sulfurreducens* strain PCA (Caccavo *et al.*, 1992) and *Shewanella putrefaciens* strain CN32 (Fredrickson *et al.*, 1998) were grown under identical conditions with fumarate as the electron acceptor, and either acetate (*G. sulfurreducens*) or lactate (*S. putrefaciens*) as the carbon and energy source. At the beginning of the experiment, cells were harvested and washed twice with sterile, anaerobic Pipes buffer (10 mM, pH 6.8) before inoculating (final cell concentration ~10^8 mL^{-1}) into 500 mL of sterile, anaerobic Pipes buffer (10 mM, pH 6.8). The buffer contained either 8 g L^{-1} hematite or 4.5 g L^{-1} goethite, and had been previously bubbled with O_2-free H_2, which served as the only energy source for Fe(III) reduction. Minimal, non-growth conditions were employed to avoid precipitation of carbonate- and phosphate-containing Fe minerals, which would hamper interpretation of the isotopic data. The absence of these phases in the experiments was confirmed by XRD analysis of the solid products and inspection of TEM images. The bottles were incubated at 30 °C in the dark, and all sampling was carried out inside an anaerobic chamber (Coy Products, Grass Lake, MI, USA).

Sampling and extraction procedures

Subsamples of the reaction slurries were collected periodically over the course of ~280 days and centrifuged to remove the aqueous fraction. The remaining solids were extracted for 1 h using 1 M Na-acetate buffer (pH 4.85) to remove the majority of sorbed Fe(II) without dissolving any underlying Fe(III); the lack of dissolution of any ferric oxide in this step was confirmed through Fe(II) and total Fe measurements, which showed that all Fe in the Na-acetate wash was Fe(II) within analytical uncertainties. Fe(II) and total Fe concentrations were measured using Ferrozine (Stookey, 1970), and Fe(III) concentrations were determined by difference. A second extraction was then performed using 0.5 M HCl to remove any remaining sorbed Fe(II), and to dissolve a small amount of the ferric oxide surface. All samples were passed through 0.2 μm filters, and aqueous and Na-acetate fractions were acidified with HCl to a final concentration of ~0.5 M. To check the reproducibility of these measurements in mixed Fe(II)/Fe(III) systems, a series of test solutions that contained between 50 and 90% Fe(II) were prepared. Five replicate Ferrozine analyses of each solution showed that the percentages of Fe(II) out of total Fe were consistent within ±1.5% (2σ), and we take this to be the average uncertainty in our Fe(II) and Fe(III) determinations.

Fe isotope measurements and control tests

All $Fe(II)_{aq}$, Na-acetate, and 0.5 M HCl fractions were purified using anion-exchange chromatography, followed by Fe isotope measurements using a multicollector inductively coupled plasma mass spectrometer, as previously described (Beard *et al.*, 2003a). Data are reported as $^{56}Fe/^{54}Fe$ ratios relative to the average of igneous rocks in standard δ notation, in units of per mil (‰):

$$\delta^{56}Fe = \left[\frac{^{56}Fe/^{54}Fe_{sample}}{^{56}Fe/^{54}Fe_{IgRxs}} - 1\right]10^3 \qquad (1)$$

The Fe isotope fractionation between two phases or species A and B is defined as:

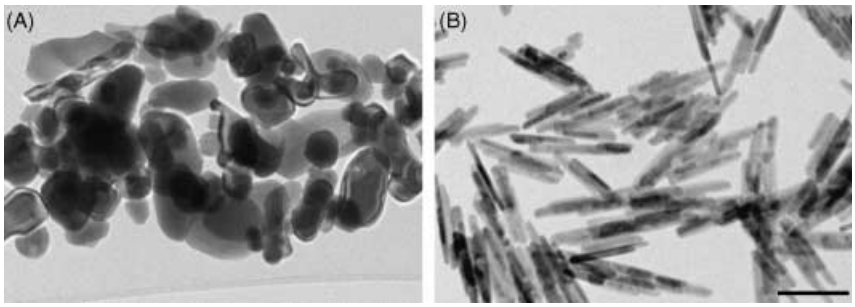

Fig. 2 TEM images of the hematite (A) and goethite (B) starting materials magnified ×75 000. Scale bars are 200 nm.

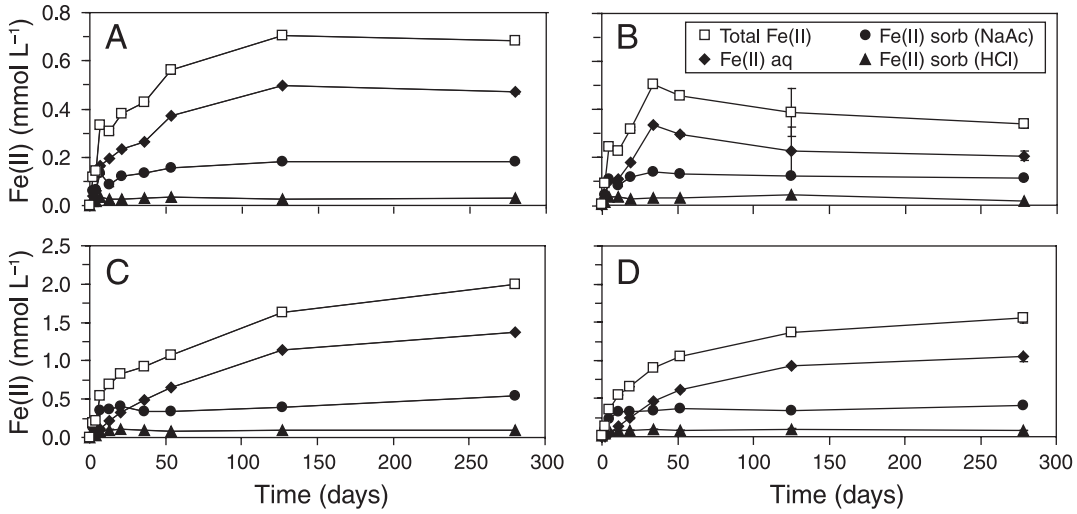

Fig. 3 Fe(II) produced during reduction of hematite by *Geobacter sulfurreducens* (A) and *Shewanella putrefaciens* (B), and goethite reduction by *G. sulfurreducens* (C) and *S. putrefaciens* (D). At each time point, $Fe(II)_{aq}$ was removed, followed by extraction of the majority of $Fe(II)_{sorb}$ with pH 4.85 Na-acetate. The remaining $Fe(II)_{sorb}$ was extracted using 0.5 M HCl. Total Fe(II) is the sum of $Fe(II)_{aq}$ and $Fe(II)_{sorb}$ in the Na-acetate and HCl extractions. Error bars show standard deviations of triplicate measurements. Fe(III) recovered in the 0.5 M HCl extractions is not shown. Data from Tables 2–5.

$$\Delta^{56}Fe_{A-B} = \delta^{56}Fe_A - \delta^{56}Fe_B \quad (2)$$

following standard practice. Measured external precision in δ^{56}Fe values is ±0.05‰ (1σ) based on replicate analyses and standards. Approximately one third of the samples from a particular reaction bottle were analysed more than once. On the igneous rock scale, the δ^{56}Fe value of the IRMM-014 standard is −0.09‰ (Beard *et al.*, 2003a).

The hematite and goethite starting materials were partially dissolved using 0.5 M HCl for varying lengths of time, and δ^{56}Fe values of the dissolved and solid fractions were measured to check that the reagents were isotopically homogeneous. Complete dissolution of bulk samples using 7 M HCl indicated that the initial δ^{56}Fe value of the hematite was +0.26‰, and that of the goethite was +0.14‰ (Table 1). To verify that the 1 M Na-acetate that was used in our extractions to sample $Fe(II)_{sorb}$ did not introduce an Fe isotope fractionation, extraction tests were performed in abiological systems of $Fe(II)_{aq}$ and hematite using either 0.05 M HCl or 1 M Na-acetate (pH 4.85). Both sets of extractions removed a similar amount of $Fe(II)_{sorb}$, and measured δ^{56}Fe values were within ~0.1‰ of each other (data not shown).

RESULTS

Comparison of hematite and goethite reduction

Despite their fine particle size (Fig. 2), only a small fraction of either ferric oxide was reduced over the course of ~280 days. *S. putrefaciens* and *G. sulfurreducens* reduced approximately 0.5% and 0.7% of the hematite, and 3.1% and 4.0% of the available goethite, respectively (Fig. 3; Tables 2–5). Although $Fe(II)_{aq}$ appears to decrease in the second half of the time course in the *S. putrefaciens*/hematite reaction bottle, we suspect that this is the result of sampling error at a single time point at the end of the experiment. Overall, the two species reduced similar amounts of each oxide material when studied under nearly identical conditions, indicating that the extent and rate of reduction was primarily controlled by substrate and not by bacterial species.

The extraction with pH 4.85 Na-acetate recovered almost exclusively Fe(II), which accounted for the majority of $Fe(II)_{sorb}$ (Tables 2–5). The subsequent 0.5 M HCl extraction always removed a mixture of Fe(II) and Fe(III), ranging from 4% to 80% Fe(III). We assume that the Fe(II) recovered in the 0.5 M HCl extraction is $Fe(II)_{sorb}$ that was not extracted by the Na-acetate, although it is possible that a small portion of this Fe(II) may be located within the oxide structure, perhaps as a result of electron transfer from $Fe(II)_{sorb}$ to the bulk oxide (Williams & Scherer, 2004; Silvester *et al.*, 2005). To facilitate interpretation of the isotope data, we assume that Fe(II) recovered in the 0.5 M HCl extractions has the same δ^{56}Fe value as $Fe(II)_{sorb}$ liberated in the Na-acetate extractions; as discussed below, this assumption is justified based on the consistency of the Fe isotope fractionations for the samples and the lack of correlation between isotopic fractionation and the proportion of Fe(II) in the 0.5 M HCl.

The Fe(II) sorption isotherms are distinct for the two oxides, commensurate with their different surface areas (Fig. 4). Sorption data for the *G. sulfurreducens* and *S. putrefaciens* experiments overlap, indicating no significant differences based on bacterial species. Over the range of $Fe(II)_{aq}$ contents of our study, between two and six times more Fe(II) was sorbed to goethite as compared to hematite, at a given $Fe(II)_{aq}$

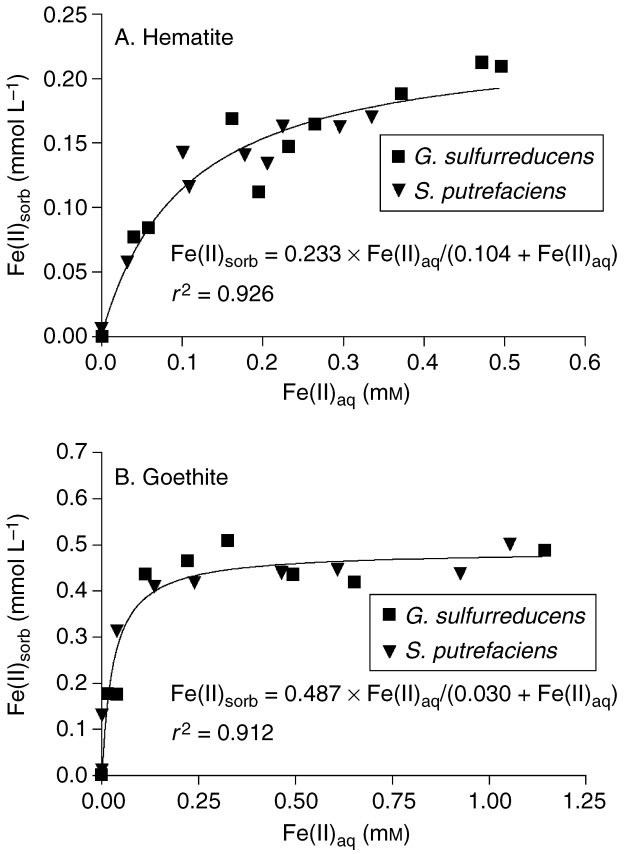

Fig. 4 Sorption isotherms. $Fe(II)_{aq}$ – $Fe(II)_{sorb}$ concentrations for the hematite (A) and goethite (B) reduction experiments. The solid lines show nonlinear least-squares regression fits of the data to a Langmuir isotherm equation: $Fe(II)_{sorb} = Fe(II)_{sorb,max} \times Fe(II)_{aq}/(K_{Fe(II)sorb} + Fe(II)_{aq})$, where $Fe(II)_{sorb,max}$ is the maximum concentration of $Fe(II)_{sorb}$, and $K_{Fe(II)sorb}$ is the $Fe(II)_{aq}$ concentration at which $Fe(II)_{sorb} = 0.5Fe(II)_{sorb,max}$. Data from Tables 2–5.

content, consistent with the ~5.5 times greater surface area for goethite.

Fe isotope changes during hematite reduction

The δ^{56}Fe values measured for $Fe(II)_{aq}$ and $Fe(II)_{sorb}$ produced by *G. sulfurreducens* have been previously reported (Crosby *et al.*, 2005), but are duplicated in Tables 3 and 5 to aid comparison. The new results for *S. putrefaciens* (Tables 2 and 4) show that the two species produced very similar isotopic fractionations in this head-to-head comparison (Fig. 5). Both species generate $Fe(II)_{aq}$ that has δ^{56}Fe values that are initially ~2‰ lower than the hematite substrate, and over the course of the experiment the δ^{56}Fe values gradually increase to values ~1‰ lower than the hematite substrate (Fig. 5A,B). Likewise, at the start of the experiment, $Fe(II)_{sorb}$ extracted using Na-acetate had δ^{56}Fe values ~1.6‰ lower than the hematite, and over time these values increase by ~0.6–0.8‰ (Fig. 5A,B).

It is noteworthy that for both bacterial species, the δ^{56}Fe values for $Fe(II)_{aq}$ and $Fe(II)_{sorb}$ are always at least 0.75‰ lower than the hematite substrate. Because this is a closed system, there must be a reservoir of Fe that has δ^{56}Fe values that are greater than those of the hematite starting materials to satisfy isotopic mass balance. The 0.5 M HCl extractions provide insight into this required high-δ^{56}Fe component. Because this set of extractions contains a mixture of Fe(II) and Fe(III), which is interpreted to reflect any remaining $Fe(II)_{sorb}$, as well as dissolution of the outer layers of the underlying hematite, we infer that the 0.5 M HCl extractions contain a mixture of Fe isotope compositions that are associated with the Fe(II) and Fe(III) components measured in solution. At all time points, the δ^{56}Fe values of the 0.5 M HCl extraction are similar to or higher than those of the hematite substrate (Fig. 5A,B). This suggests that a reactive phase or 'layer', $Fe(III)_{reac}$, is forming at the hematite surface that is isotopically distinct from $Fe(II)_{aq}$, $Fe(II)_{sorb}$, and the underlying hematite substrate.

Fe isotope changes during goethite reduction

During goethite reduction by *S. putrefaciens*, the difference between the δ^{56}Fe value of the initial goethite and $Fe(II)_{aq}$ begins at –0.95‰, increases to –0.65‰, and decreases again to –1.55‰ (Fig. 5C,D). These values, as well as the general temporal trend, were very similar in the companion experiment using *G. sulfurreducens*. The δ^{56}Fe values of $Fe(II)_{sorb}$ in the Na-acetate extractions also rise initially and then decrease. In contrast to experiments with hematite, however, Fe(II) sorbed to goethite was, on average, isotopically similar to the bulk goethite. Thus, the δ^{56}Fe values of $Fe(II)_{sorb}$ cannot provide the required isotopic mass balance for the low-δ^{56}Fe $Fe(II)_{aq}$, suggesting that another Fe reservoir must be present in the system. As in the hematite experiments, the 0.5 M HCl extractions appear to sample this required high-δ^{56}Fe phase. In the *S. putrefaciens* experiment, the Fe recovered in the 0.5 M HCl extractions has δ^{56}Fe values that are 0.24–0.86‰ higher than that of the initial goethite substrate (Fig. 5C,D). This is consistent with results from *G. sulfurreducens*, in which Fe in the 0.5 M HCl extraction is 0.08–0.97‰ higher than the goethite starting material (Fig. 5C).

Calculation of δ^{56}Fe values for the Fe(III) end-member in the 0.5 M HCl extractions

Following Crosby *et al.* (2005), we will assume that the Fe isotope compositions of the 0.5 M HCl extractions reflect a mixture of δ^{56}Fe values for pure-Fe(II) and Fe(III) components, where the δ^{56}Fe values of the Fe(II) component in the 0.5 M HCl extraction are the same as $Fe(II)_{sorb}$ obtained in the Na-acetate wash. There are, however, other possible interpretations for this component. For example, Fe(II) in the 0.5 M HCl extraction may reflect Fe that has been dispersed in the oxide,

Table 1 Initial Fe isotope compositions of ferric oxide starting materials and tests for isotopic homogeneity

		Analyses				Average of replicates			
Sample	Aliquot*	δ^{56}Fe	2 – SE†	δ^{57}Fe	2 – SE	δ^{56}Fe	1 – SD‡	δ^{57}Fe	1 – SD
Hematite starting material									
	1	0.22	0.06	0.36	0.03	0.26	0.04	0.40	0.05
	repeat	0.29	0.04	0.41	0.04				
	2	0.29	0.07	0.40	0.03				
	repeat	0.31	0.06	0.48	0.03				
	3	0.22	0.05	0.42	0.05				
	4	0.23	0.03	0.34	0.03				
Hematite partial dissolutions									
2.0% dissolved, aqueous		0.35	0.04	0.54	0.03	0.31	0.06	0.46	0.11
		0.27	0.06	0.39	0.05				
2.0% dissolved, solids		0.15	0.04	0.26	0.03	0.19	0.06	0.31	0.07
		0.24	0.05	0.36	0.04				
4.7% dissolved, aqueous		0.28	0.05	0.41	0.03	0.29	0.02	0.42	0.01
		0.30	0.06	0.43	0.05				
4.7% dissolved, solids		0.16	0.03	0.30	0.03	0.22	0.09	0.40	0.14
		0.28	0.04	0.49	0.04				
11.1% dissolved, aqueous		0.22	0.04	0.23	0.09	0.25	0.05	0.29	0.08
		0.29	0.05	0.35	0.04				
11.1% dissolved, solids		0.08	0.03	0.20	0.03	0.18	0.09	0.27	0.07
		0.18	0.02	0.29	0.02				
		0.27	0.04	0.32	0.04				
21.1% dissolved, aqueous		0.19	0.07	0.21	0.04	0.18	0.01	0.30	0.01
		0.18	0.05	0.31	0.05				
21.1% dissolved, solids		0.16	0.04	0.26	0.04	0.22	0.09	0.33	0.09
		0.28	0.05	0.40	0.04				
45.4% dissolved, aqueous		0.34	0.05	0.48	0.03	0.27	0.06	0.42	0.05
		0.23	0.06	0.40	0.05				
		0.25	0.08	0.39	0.03				
45.4% dissolved, solids		0.23	0.02	0.34	0.02	0.22	0.01	0.32	0.03
		0.21	0.04	0.30	0.04				
Goethite starting material									
	1	0.10	0.04	0.14	0.03	0.14	0.06	0.21	0.10
	repeat	0.15	0.07	0.23	0.04				
	2	0.24	0.07	0.35	0.06				
	3	0.16	0.03	0.25	0.04				
	4	0.07	0.02	0.09	0.03				
Goethite partial dissolutions									
0.7% dissolved, aqueous		–0.01	0.03	–0.03	0.03	–0.04	0.03	–0.05	0.02
		–0.06	0.05	–0.06	0.03				
0.7% dissolved, solids		0.14	0.03	0.22	0.05	0.12	0.03	0.17	0.07
		0.10	0.05	0.13	0.03				
1.2% dissolved, aqueous		–0.03	0.03	–0.05	0.03	–0.02	0.01	–0.06	0.02
		0.01	0.05	–0.07	0.05				
1.2% dissolved, solids		0.06	0.04	0.08	0.03	0.08	0.03	0.12	0.06
		0.10	0.06	0.16	0.07				
2.0% dissolved, aqueous		0.08	0.05	0.10	0.03	0.05	0.04	0.06	0.06
		0.02	0.04	0.02	0.04				
2.0% dissolved, solids		0.09	0.03	0.18	0.03	0.09	0.00	0.17	0.01
		0.09	0.05	0.17	0.04				
3.9% dissolved, aqueous		0.18	0.03	0.29	0.03	0.14	0.05	0.24	0.07
		0.11	0.04	0.18	0.04				
3.9% dissolved, solids		0.10	0.03	0.15	0.03	0.10	0.00	0.13	0.02
		0.10	0.04	0.12	0.04				
9.5% dissolved, aqueous		0.21	0.03	0.30	0.02	0.21	0.00	0.26	0.06
		0.21	0.05	0.22	0.03				
9.5% dissolved, solids		0.23	0.03	0.33	0.03	0.17	0.08	0.24	0.14
		0.12	0.04	0.14	0.04				

*Different aliquots are from the same sample but were separately processed through anion-exchange chromatography, whereas repeats are different isotopic analyses of the same aliquot.

†2 – SE is the internal standard error based on forty 10-s on-peak integrations taken for each analysis.

‡1 – SD is the standard deviation of multiple measurements of the same sample (either repeats of one aliquot or different aliquots processed separately through anion exchange chromatography).

Table 2 Fe isotope compositions of aqueous, Na-acetate (NaAc) and 0.5 M HCl (HCl) fractions for *Shewanella putrefaciens* reduction of hematite

Sample	Aliquot	Day	Fe(II) (mM)	error* (mM)	Fe(III) (mM)	error (mM)	Analyses†				Average of replicates			
							δ^{56}Fe	2 – SE	δ^{57}Fe	2 – SE	δ^{56}Fe	1 – SD	δ^{57}Fe	1 – SD
Aqueous		0.0	0.000	0.000	0.000	0.000								
NaAc		0.0	0.001	0.001	0.000	0.001								
HCl	1	0.0	0.005	0.001	0.028	0.001	–0.18	0.06	–0.16	0.04	–0.16	0.04	–0.19	0.05
	repeat						–0.13	0.02	–0.23	0.02				
Aqueous	1	2.0	0.032	0.004	0.001	0.008	–1.78	0.04	–2.66	0.03				
NaAc	1	2.0	0.043	0.001	0.000	0.001	–1.32	0.02	–1.98	0.03				
HCl	1	2.0	0.014	0.001	0.033	0.001	0.31	0.02	0.41	0.03				
Aqueous	1	4.8	0.101	0.002	0.042	0.002	–1.44	0.04	–2.17	0.03				
NaAc	1	4.8	0.108	0.001	0.003	0.001	–1.22	0.02	–1.81	0.02	–1.19	0.04	–1.77	0.06
	repeat						–1.16	0.06	–1.72	0.06				
HCl	1	4.8	0.035	0.002	0.033	0.003	0.26	0.03	0.37	0.02				
Aqueous	1	10.7	0.109	0.002	0.083	0.002	–1.43	0.02	–2.21	0.03				
NaAc	1	10.7	0.081	0.002	0.003	0.003	–1.23	0.06	–1.86	0.05				
HCl	1	10.7	0.035	0.001	0.033	0.001	0.19	0.04	0.26	0.04				
Aqueous	1	18.7	0.178	0.002	0.023	0.002	–1.24	0.05	–1.80	0.06				
NaAc	1	18.7	0.116	0.000	0.011	0.002	–1.10	0.02	–1.55	0.04				
HCl	1	18.7	0.025	0.005	0.037	0.006	0.48	0.02	0.70	0.03				
Aqueous	1	33.8	0.335	0.002	0.018	0.005	–1.15	0.05	–1.72	0.06				
NaAc	1	33.8	0.140	0.003	0.004	0.004	–1.08	0.06	–1.59	0.06				
HCl	1	33.8	0.030	0.001	0.113	0.001	0.84	0.03	1.23	0.02				
Aqueous	1	51.7	0.296	0.007	0.013	0.007	–1.28	0.02	–1.97	0.03	–1.34	0.09	–2.01	0.06
	repeat						–1.40	0.06	–2.06	0.04				
NaAc	1	51.7	0.132	0.001	0.018	0.002	–1.20	0.04	–1.82	0.05	–1.16	0.06	–1.71	0.15
	repeat						–1.11	0.02	–1.60	0.02				
HCl	1	51.7	0.031	0.003	0.025	0.004	0.52	0.04	0.78	0.04				
Aqueous	1	125	0.225	0.101	0.014	0.137	–1.18	0.04	–1.81	0.04				
NaAc	1	125	0.121	0.003	0.009	0.005	–1.05	0.04	–1.57	0.04				
HCl	1	125	0.042	0.003	0.014	0.003	0.16	0.03	0.18	0.03				
Aqueous	1	278	0.206	0.019	0.032	0.022	–0.71	0.02	–1.01	0.02	–0.71	0.00	–1.02	0.01
	repeat						–0.72	0.05	–1.03	0.03				
NaAc	1	278	0.115	0.001	0.001	0.002	–0.45	0.05	–0.70	0.04	–0.49	0.06	–0.71	0.01
	repeat						–0.53	0.02	–0.72	0.02				
HCl	1	278	0.019	0.003	0.021	0.003	0.86	0.05	1.23	0.02	0.81	0.07	1.20	0.04
	repeat						0.77	0.02	1.18	0.02				

*Fe(II) and total Fe were measured using Ferrozine, and Fe(III) was determined by difference. Errors are based on the standard deviation of triplicate measurements, and errors for Fe(III) use the square root of the sum of the squares of Fe(II) and total Fe errors.

†Errors for isotopic measurements are described in Table 1.

as a result of spontaneous electron transfer from sorbed Fe(II) to the ferric oxide surface (Rosso *et al.*, 2003a; Williams & Scherer, 2004; Silvester *et al.*, 2005). In addition, it is possible that the Fe(II) recovered in the 0.5 M HCl extraction is part of a new mixed-valence Fe precipitate that formed at the oxide surface. We did not see any evidence of a new phase in TEM images of the oxide materials, and other recent studies using Mössbauer or EXAFS spectroscopy found no evidence for formation of new mineral phases such as magnetite or green rust when Fe(II) adsorbed to hematite or goethite (Kukkadapu *et al.*, 2001; Hansel *et al.*, 2004; Williams & Scherer, 2004; Silvester *et al.*, 2005). The contrast in δ^{56}Fe values for $Fe(II)_{aq}$ and Fe in the HCl extractions ranges from –1.0 to –2.2‰ (Tables 2–5), which can be described as a $\Delta^{56}Fe_{Fe(II)aq-HCl}$ 'fractionation', is far from the +0.25‰ $Fe(II)_{aq}$-green rust fractionation measured at room temperature by Wiesli *et al.* (2004), providing strong evidence that the HCl extractions do not represent dissolution of green rust of mixed Fe(II)–Fe(III) stoichiometry.

Although the experimentally determined $Fe(II)_{aq}$–magnetite fractionation (–1.3‰ at room temperature; Johnson *et al.*, 2005) overlaps the range of the measured $\Delta^{56}Fe_{Fe(II)aq-HCl}$ 'fractionation' for some samples, the $Fe(II)/Fe_{Total}$ ratios for such extractions are 0.8–0.9 (Tables 2–5), which is far from that required by the stoichiometry of magnetite ($Fe(II)/Fe_{Total} = 0.33$), indicating that the 0.5 M HCl extractions do not reflect dissolution of magnetite. Based on these results, and the lack of evidence by XRD or TEM for formation of a mixed-valence Fe precipitate, we conclude that the HCl extractions most likely recovered a mixture of $Fe(II)_{sorb}$ that remained after the NaAc extraction, together with Fe(III) that was dissolved from the oxide substrate.

Table 3 Fe isotope compositions of aqueous, Na-acetate (NaAc) and 0.5 M HCl (HCl) fractions for *Geobacter sulfurreducens* reduction of hematite

Sample	Aliquot	Day	Fe(II) (mM)	error* (mM)	Fe(III) (mM)	error (mM)	Analyses†				Average of replicates			
							δ^{56}Fe	2 – SE	δ^{57}Fe	2 – SE	δ^{56}Fe	1 – SD	δ^{57}Fe	1 – SD
Aqueous		0.00	0.001	0.0022	0.000	0.0032								
NaAc		0.00	0.000	0.0000	0.000	0.0000								
HCl		0.00	0.000	0.0000	0.000	0.0000								
Aqueous	1	2.00	0.041	0.0022	0.000	0.0032	–1.81	0.05	–2.68	0.04	–1.83	0.03	–2.67	0.01
	repeat						–1.85	0.06	–2.66	0.03				
NaAc	1	2.00	0.060	0.0010	0.000	0.0018	–1.52	0.07	–2.19	0.03	–1.46	0.09	–2.12	0.10
	2						–1.40	0.03	–2.06	0.02				
HCl	1	2.00	0.017	0.0000	0.031	0.0000	0.34	0.04	0.42	0.05	0.30	0.05	0.44	0.02
	2						0.27	0.03	0.45	0.02				
Aqueous	1	4.00	0.059	0.0022	0.000	0.0032	–1.59	0.03	–2.34	0.03				
NaAc	1	4.00	0.065	0.0022	0.001	0.0027	–1.06	0.03	–1.47	0.03				
HCl	1	4.00	0.019	0.0000	0.038	0.0012	0.34	0.03	0.44	0.03	0.35	0.01	0.51	0.09
	2						0.35	0.03	0.57	0.02				
Aqueous	1	6.83	0.163	0.0022	0.041	0.0022	–1.46	0.03	–2.14	0.02	–1.45	0.02	–2.12	0.04
	repeat						–1.44	0.03	–2.09	0.04				
NaAc	1	6.83	0.132	0.0039	0.004	0.0044	–1.07	0.02	–1.61	0.03	–1.00	0.10	–1.51	0.14
	repeat						–0.94	0.07	–1.41	0.05				
HCl	1	6.83	0.037	0.0010	0.030	0.0018	0.39	0.04	0.53	0.03	0.30	0.12	0.37	0.23
	repeat						0.21	0.06	0.21	0.06				
Aqueous	1	12.7	0.196	0.0077	0.024	0.0104	–1.23	0.04	–1.86	0.04	–1.30	0.11	–1.93	0.11
	2						–1.38	0.06	–2.01	0.04				
NaAc	1	12.7	0.087	0.0092	0.003	0.0127	–0.91	0.03	–1.36	0.04	–0.93	0.03	–1.33	0.05
	2						–0.96	0.03	–1.30	0.03				
HCl	1	12.7	0.025	0.0029	0.021	0.0055	0.35	0.03	0.56	0.03	0.33	0.12	0.51	0.18
	2						0.21	0.03	0.30	0.03				
	repeat						0.45	0.04	0.66	0.03				
Aqueous	1	20.7	0.233	0.0022	0.018	0.0052	–1.32	0.09	–1.93	0.04	–1.29	0.04	–1.92	0.02
	repeat						–1.27	0.03	–1.91	0.03				
NaAc	1	20.7	0.123	0.0006	0.009	0.0030	–0.83	0.03	–1.18	0.03	–0.86	0.04	–1.22	0.07
	2						–0.89	0.05	–1.27	0.02				
HCl	1	20.7	0.025	0.0006	0.039	0.0008	0.57	0.06	0.79	0.03	0.63	0.05	0.91	0.11
	2						0.67	0.03	0.99	0.03				
	repeat						0.64	0.04	0.95	0.04				
Aqueous	1	35.8	0.265	0.0000	0.014	0.0047	–1.36	0.09	–2.02	0.04				
NaAc	1	35.8	0.135	0.0006	0.010	0.0013	–0.90	0.04	–1.27	0.05	–0.93	0.04	–1.37	0.13
	2						–0.96	0.03	–1.46	0.03				
HCl	1	35.8	0.030	0.0010	0.118	0.0011	0.94	0.04	1.40	0.04	0.86	0.07	1.25	0.13
	2						0.80	0.03	1.15	0.03				
	repeat						0.84	0.04	1.21	0.05				
Aqueous	1	53.7	0.372	0.0138	0.018	0.0207	–1.17	0.07	–1.76	0.06	–1.15	0.02	–1.78	0.04
	2						–1.14	0.06	–1.81	0.04				
NaAc	1	53.7	0.155	0.0019	0.000	0.0030	–0.90	0.04	–1.34	0.03				
HCl	1	53.7	0.033	0.0025	0.020	0.0040	0.50	0.05	0.76	0.05				
Aqueous	1	127	0.496	0.0117	0.016	0.0194	–1.13	0.03	–1.67	0.03	–1.07	0.09	–1.57	0.14
	repeat						–1.00	0.03	–1.47	0.03				
NaAc	1	127	0.182	0.0029	0.024	0.0039	–0.50	0.03	–0.82	0.03	–0.59	0.07	–0.89	0.07
	repeat						–0.59	0.04	–0.84	0.04				
	2						–0.68	0.03	–0.97	0.03				
	repeat						–0.59	0.04	–0.92	0.04				
HCl	1	127	0.027	0.0015	0.015	0.0075	0.68	0.04	1.09	0.03	0.68	0.01	1.02	0.10
	2						0.68	0.06	0.95	0.05				
Aqueous	1	280	0.472	0.0077	0.050	0.0193	–0.84	0.03	–1.20	0.03				
NaAc	1	280	0.182	0.0031	0.006	0.0039	–0.74	0.03	–1.10	0.03				
HCl	1	280	0.031	0.0017	0.021	0.0034	0.67	0.03	0.95	0.04				

Analysis methods and error calculations as in Tables 1 and 2.

Table 4 Fe isotope compositions of aqueous, Na-acetate (NaAc) and 0.5 M HCl (HCl) fractions for *Shewanella putrefaciens* reduction of goethite

Sample	Aliquot	Day	Fe(II) (mM)	error (mM)	Fe(III) (mM)	error (mM)	Analyses				Average of replicates			
							δ^{56}Fe	2 – SE	δ^{57}Fe	2 – SE	δ^{56}Fe	1 – SD	δ^{57}Fe	1 – SD
Aqueous		0.0	0.000	0.000	0.000	0.000								
NaAc		0.0	0.000	0.000	0.000	0.000								
HCl		0.0	0.012	0.000	0.011	0.000	–0.38	0.04	–0.53	0.04				
Aqueous	1	2.0	0.000	0.000	0.000	0.000								
NaAc	1	2.0	0.089	0.001	0.000	0.001	–0.14	0.03	–0.29	0.03				
HCl	1	2.0	0.041	0.000	0.008	0.000	0.39	0.03	0.56	0.03				
Aqueous	1	4.8	0.038	0.000	0.035	0.000	–0.81	0.05	–1.17	0.04				
NaAc	1	4.8	0.237	0.002	0.006	0.002	0.06	0.05	0.06	0.03				
HCl	1	4.8	0.075	0.001	0.010	0.001	0.55	0.03	0.84	0.02	0.52	0.04	0.79	0.07
	repeat						0.49	0.03	0.74	0.02				
Aqueous	1	10.7	0.136	0.002	0.031	0.002	–0.47	0.06	–0.65	0.08	–0.53	0.08	–0.74	0.13
	repeat						–0.58	0.02	–0.83	0.01				
NaAc	1	10.7	0.330	0.002	0.005	0.002	0.22	0.03	0.29	0.04				
HCl	1	10.7	0.079	0.003	0.009	0.005	0.57	0.11	0.89	0.03				
Aqueous	1	18.7	0.239	0.004	0.022	0.006	–0.53	0.05	–0.82	0.04	–0.54	0.01	–0.81	0.02
	repeat						–0.54	0.03	–0.79	0.02				
NaAc	1	18.7	0.332	0.002	0.010	0.005	0.28	0.10	0.40	0.06				
HCl	1	18.7	0.086	0.001	0.020	0.001	0.69	0.05	1.01	0.06				
Aqueous	1	33.8	0.464	0.004	0.019	0.005	–0.51	0.04	–0.72	0.04				
NaAc	1	33.8	0.344	0.003	0.011	0.003	0.32	0.05	0.51	0.03				
HCl	1	33.8	0.095	0.001	0.066	0.001	1.00	0.03	1.50	0.02				
Aqueous	1	51.7	0.609	0.004	0.014	0.004	–0.69	0.04	–0.95	0.04	–0.61	0.10	–0.89	0.09
	repeat						–0.54	0.03	–0.83	0.04				
NaAc	1	51.7	0.366	0.001	0.007	0.002	0.33	0.05	0.51	0.03				
HCl	1	51.7	0.081	0.002	0.005	0.003	0.83	0.03	1.20	0.02				
Aqueous	1	125	0.926	0.012	0.010	0.019	–1.04	0.05	–1.54	0.05	–1.08	0.06	–1.60	0.09
	repeat						–1.12	0.05	–1.66	0.05				
NaAc	1	125	0.338	0.008	0.055	0.012	–0.17	0.06	–0.15	0.04				
HCl	1	125	0.099	0.004	0.004	0.004	0.59	0.03	0.91	0.03	0.55	0.06	0.83	0.12
	repeat						0.50	0.03	0.74	0.02				
Aqueous	1	278	1.054	0.065	0.039	0.079	–1.34	0.05	–2.00	0.04	–1.41	0.09	–2.11	0.15
	repeat						–1.47	0.03	–2.21	0.05				
NaAc	1	278	0.416	0.004	0.012	0.008	–0.32	0.02	–0.51	0.02				
HCl	1	278	0.085	0.001	0.013	0.002	0.39	0.02	0.61	0.01	0.38	0.01	0.59	0.02
	repeat						0.38	0.02	0.57	0.03				

Analysis methods and error calculations as in Tables 1 and 2.

We next examine the assumption that the δ^{56}Fe value of the Fe(II) component in the HCl extractions is equal to that of the NaAc extraction, an assumption that is important in constructing the HCl mixing lines discussed below. If there was a systematic difference between δ^{56}Fe values for Fe(II) in the HCl extraction and NaAc extractions, this would produce a linear mixing correlation between the measured $\Delta^{56}Fe_{Fe(II)aq-Fe(II)sorb}$ fractionation and the amount of $Fe(II)_{sorb}$ removed by NaAc extraction relative to the total $Fe(II)_{sorb}$ inventory determined by NaAc + HCl. This is not, however, observed: the proportion of $Fe(II)_{sorb}$ in the NaAc extraction varied from 0.68 to 0.87, and linear regression relative to the measured $\Delta^{56}Fe_{Fe(II)aq-Fe(II)sorb}$ fractionation produced low correlation coefficients ($R^2 = 0.08$–0.47). A second test comes from considering the inferred fractionation between the Fe(III) component in the 0.5 M HCl extraction and $Fe(II)_{aq}$ as a function of the percentage Fe(II) in the extraction. As will be shown below, the inferred $Fe(III)_{reac} - Fe(II)_{aq}$ fractionation is relatively constant over a wide range of Fe(II) proportions (~20–80%) in the HCl extractions (hematite experiments) using the assumption that the δ^{56}Fe value of the Fe(II) component in the HCl extraction is equal to that of $Fe(II)_{sorb}$ in the NaAc extraction; if this assumption were invalid, such relations would not be observed. These observations validate the assumption that the δ^{56}Fe value of the Fe(II) component in the HCl extraction is equal to that of $Fe(II)_{sorb}$ determined in the NaAc extraction.

The δ^{56}Fe value of the Fe(III) component in the 0.5 M HCl extractions may be calculated using a simple isotopic mass balance equation:

$$\delta^{56}Fe_{HCl} = X_{Fe(II)}\delta^{56}Fe_{Fe(II)sorb} + X_{Fe(III)}\delta^{56}Fe_{Fe(III)reac} \quad (3)$$

where X represents the mole fractions of Fe(II) and Fe(III) in the 0.5 M HCl extraction, as determined by Ferrozine measurements, and $X_{Fe(II)}$ is taken as $Fe(II)_{sorb}$ that remained after the NaAc extraction and $X_{Fe(III)}$ is interpreted to be

Table 5 Fe isotope compositions of aqueous, Na-acetate (NaAc) and 0.5 M HCl (HCl) fractions for *Geobacter sulfurreducens* reduction of goethite

Sample	Aliquot	Day	Fe(II) (mM)	error (mM)	Fe(III) (mM)	error (mM)	Analyses				Average of replicates			
							δ^{56}Fe	2 – SE	δ^{57}Fe	2 – SE	δ^{56}Fe	1 – SD	δ^{57}Fe	1 – SD
Aqueous		0.00	0.000	0.0000	0.000	0.0000								
NaAc		0.00	0.000	0.0000	0.000	0.0000								
HCl		0.00	0.000	0.0000	0.000	0.0000								
Aqueous	1	2.00	0.015	0.0000	0.000	0.0000	–0.79	0.03	–1.09	0.02				
NaAc	1	2.00	0.135	0.0040	0.001	0.0056	–0.07	0.03	–0.03	0.03				
HCl	1	2.00	0.042	0.0010	0.006	0.0018	0.65	0.03	0.96	0.03				
Aqueous	1	4.00	0.038	0.0000	0.001	0.0024	–0.54	0.04	–0.80	0.05				
NaAc	1	4.00	0.144	0.0000	0.000	0.0006	0.17	0.03	0.31	0.03				
HCl	1	4.00	0.032	0.0000	0.005	0.0000	0.67	0.03	1.05	0.03	0.73	0.08	1.07	0.03
	2						0.79	0.07	1.09	0.05				
Aqueous	1	6.83	0.113	0.0059	0.042	0.0071	–0.38	0.03	–0.57	0.03				
NaAc	1	6.83	0.349	0.0044	0.010	0.0060	0.23	0.06	0.40	0.03				
HCl	1	6.83	0.088	0.0006	0.015	0.0036	0.72	0.03	1.12	0.03	0.70	0.03	1.06	0.09
	2						0.68	0.04	1.00	0.05				
Aqueous	1	12.7	0.221	0.0044	0.034	0.0050	–0.41	0.08	–0.61	0.08				
NaAc	1	12.7	0.363	0.0115	0.013	0.0128	0.29	0.03	0.47	0.02				
HCl	1	12.7	0.102	0.0019	0.012	0.0025	0.63	0.03	0.93	0.02				
Aqueous	1	20.7	0.326	0.0038	0.024	0.0056	–0.58	0.06	–0.83	0.07				
NaAc	1	20.7	0.404	0.0011	0.006	0.0026	0.34	0.05	0.49	0.03	0.33	0.01	0.52	0.04
	2						0.32	0.03	0.54	0.03				
HCl	1	20.7	0.104	0.0006	0.013	0.0012	0.78	0.06	1.25	0.04	0.77	0.02	1.20	0.06
	2						0.75	0.02	1.16	0.02				
Aqueous	1	35.8	0.494	0.0080	0.026	0.0101	–0.37	0.03	–0.50	0.03				
NaAc	1	35.8	0.339	0.0028	0.027	0.0229	0.37	0.04	0.60	0.04				
HCl	1	35.8	0.097	0.0034	0.068	0.0035	1.16	0.07	1.86	0.05	1.11	0.07	1.79	0.10
	2						1.06	0.05	1.72	0.03				
Aqueous	1	53.7	0.654	0.0022	0.010	0.0046	–0.80	0.05	–1.20	0.04				
NaAc	1	53.7	0.344	0.0020	0.010	0.0020	0.38	0.03	0.58	0.03				
HCl	1	53.7	0.075	0.0022	0.012	0.0031	0.96	0.08	1.46	0.04				
Aqueous	1	127	1.145	0.0363	0.000	0.0378	–1.04	0.04	–1.55	0.03				
NaAc	1	127	0.390	0.0031	0.067	0.0069	–0.10	0.03	–0.18	0.02	–0.05	0.07	–0.11	0.10
	2						–0.01	0.02	–0.04	0.03				
HCl	1	127	0.098	0.0015	0.009	0.0034	0.59	0.06	0.92	0.05	0.52	0.07	0.78	0.01
	2						0.47	0.06	0.67	0.03				
	3						0.51	0.03	0.74	0.03				
Aqueous	1	280	1.366	0.0066	0.026	0.0316	–1.24	0.03	–1.70	0.04				
NaAc	1	280	0.538	0.0051	0.013	0.0114	–0.08	0.03	–0.10	0.03				
HCl	1	280	0.094	0.0020	0.013	0.0022	0.22	0.05	0.27	0.04				

Analysis methods and error calculations as in Tables 1 and 2.

Fe(III) that was dissolved from the surface of the hematite or goethite. This mixing relation is represented graphically in Fig. 6. For each time point the $\delta^{56}Fe_{Fe(II)sorb}$, as determined by the Na-acetate extraction, is plotted at $X_{Fe(II)} = 1$, and the δ^{56}Fe value measured in the Fe(II)–Fe(III) mixture in the 0.5 M HCl extraction is plotted at the corresponding $X_{Fe(II)}$ for that sample. A straight line is drawn between these two points, extrapolating to $X_{Fe(II)} = 0$ to obtain the δ^{56}Fe value of the pure Fe(III) component in the 0.5 M HCl extraction; following Crosby *et al.* (2005), we define this as $\delta^{56}Fe_{Fe(III)reac}$ to denote that this is a reactive Fe(III) component on the surface of the oxides that was open to isotopic exchange.

The best estimates of $\delta^{56}Fe_{Fe(III)reac}$ are obtained when the 0.5 M HCl extraction contains a high ratio of Fe(III) to Fe(II), as is evident from a comparison of extrapolated values in the hematite experiments, which contained a high proportion of Fe(III), to those of the goethite experiments, which contained low proportions of Fe(III) (Fig. 6). Estimating the $\delta^{56}Fe_{Fe(III)reac}$ values from the 0.5 M HCl extractions that contain a high proportion of Fe(III) will minimize any errors introduced by the assumption that the δ^{56}Fe values of the Fe(II) component in the HCl extractions are equal to those measured in the NaAc extractions. We used the Excel add-in ISOPLOT (Ludwig, 1991) to calculate the 2σ errors in $\delta^{56}Fe_{Fe(III)reac}$. In Fig. 6, the extrapolations that resulted in $\delta^{56}Fe_{Fe(III)reac}$ errors ≥1‰ are indicated with dashed lines and these were not considered further in calculating $\Delta^{56}Fe_{Fe(II)aq–Fe(III)reac}$ fractionation factors (below). Samples that had an $X_{Fe(III)}$ of 0.15 or greater generally had calculated errors for $\delta^{56}Fe_{Fe(III)reac}$ that were <1‰. Calculated $\delta^{56}Fe_{Fe(III)reac}$ values for the

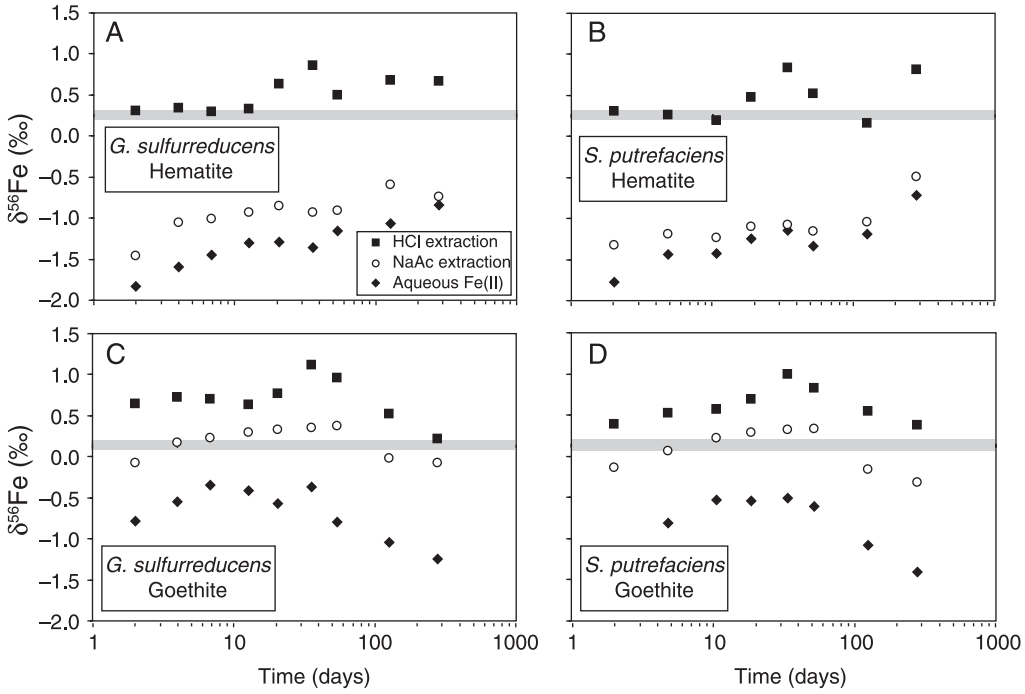

Fig. 5 Temporal variations in measured δ^{56}Fe values for aqueous Fe(II), sorbed Fe(II) in the Na-acetate extraction, and total Fe (both Fe(II) and Fe(III)) in the 0.5 M HCl extraction. The horizontal grey bars show the initial Fe isotope composition of the hematite or goethite substrate. Data from Tables 2–5.

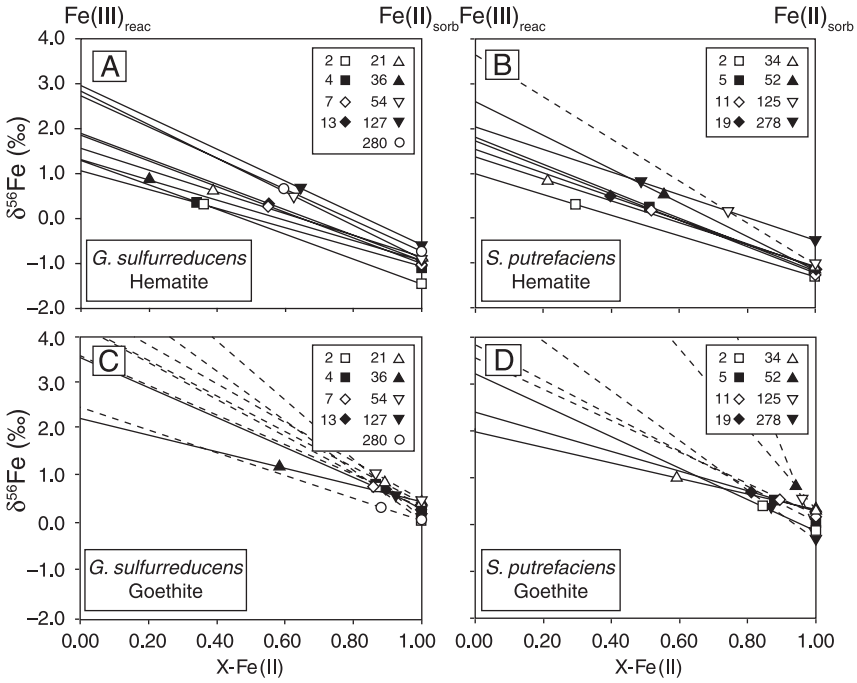

Fig. 6 Mixing diagrams illustrating calculation of Fe(III) end-member component in the 0.5 M HCl extractions, which contained mixtures of Fe(II) and Fe(III). δ^{56}Fe-$X_{Fe(II)}$ pairs for each time sample (days shown in legend) reflect those measured in the 0.5 M HCl extraction or in the Na-acetate extraction ($X_{Fe(II)} = 1.0$). In the Fe(II)–Fe(III) mixtures of the 0.5 M HCl extractions, the pure Fe(II) end member is taken as $Fe(II)_{sorb}$ ($X_{Fe(II)} = 1.0$) using the δ^{56}Fe value from the Na-acetate extraction. Extrapolation from $X_{Fe(II)} = 1.0$ through the δ^{56}Fe and $X_{Fe(II)}$ measured for the 0.5 M HCl extraction to $X_{Fe(II)} = 0.0$ allows calculation of the δ^{56}Fe values for the pure Fe(III) component in the extraction. The uncertainties in the calculated δ^{56}Fe values for the Fe(III) end member are largest when $X_{Fe(II)}$ in the 0.5 M HCl extractions are high; extrapolations that produce uncertainties ≥1.0‰ are shown in dashed lines. Data from Tables 2–5.

S. putrefaciens experiments ranged from +1.0 to +2.1‰ for hematite and +2.0 and +2.4‰ for goethite (Table 6). For the *G. sulfurreducens* experiments initially reported in Crosby *et al.* (2005), the $\delta^{56}Fe_{Fe(III)reac}$ values ranged from +1.0 to +3.0‰ for hematite, and +2.2 and +3.6‰ for goethite (Table 7).

Calculation of $Fe(II)_{aq}$ – $Fe(II)_{sorb}$ and $Fe(II)_{aq}$ – $Fe(II)_{reac}$ fractionation factors

In Fig. 7 we compare the $\Delta^{56}Fe_{Fe(II)aq-Fe(II)sorb}$ and $\Delta^{56}Fe_{Fe(II)aq-Fe(III)reac}$ fractionations obtained for reduction of

Table 6 Reactive Fe species and calculated Fe isotope fractionations for *Shewanella putrefaciens*

Day	Reduction rate % Fe(II)/d*	$Fe(II)_{aq}$ mM†	$Fe(II)_{sorb}$ mM	$Fe(III)_{reac}$ mM	Tot Reac Fe Pool mM‡	X-$Fe(II)_{aq}$§	X-$Fe(II)_{sorb}$	X-$Fe(III)_{reac}$	$\Delta Fe(II)_{aq} - Fe(II)_{sorb}$	2σ error¶	$\Delta Fe(II)_{aq} - Fe(III)_{reac}$	2σ error
Hematite experiment												
2.0	3.62×10^{-2}	0.0320	0.0576	0.163	0.252	0.13	0.23	0.65	–0.46	0.14	–2.77	0.18
4.8	2.67×10^{-2}	0.1011	0.1427	0.291	0.535	0.19	0.27	0.54	–0.25	0.14	–3.24	0.33
10.7	1.40×10^{-2}	0.1087	0.1161	0.272	0.497	0.22	0.23	0.55	–0.20	0.14	–3.15	0.25
18.7	5.85×10^{-3}	0. 1778	0.1407	0.305	0.624	0.29	0.23	0.49	–0.14	0.14	–2.77	0.42
33.8	1.12×10^{-3}	0.3352	0. 1702	0.441	0.946	0.35	0.18	0.47	–0.07	0.14	–2.51	0.42
51.7	1.59×10^{-4}	0.2955	0.1625	0.503	0.961	0.31	0.17	0.52	–0.18	0.14	–3.94	0.51
125.0	5.32×10^{-8}	0.2252	0.1628	0.345	0.733	0.31	0.22	0.47	–0.14	0.14		
278.0	2.95×10^{-15}	0.2060	0.1340	0.148	0.488	0.42	0.27	0.30	–0.22	0.14	–2.75	0.38
Goethite experiment												
2.0	4.24×10^{-2}		0.1302									
4.8	3.89×10^{-2}	0.0384	0.3128	0.030	0.381	0.10	0.82	0.08	–0.87	0.14		
10.7	3.24×10^{-2}	0.1356	0.4091	0.034	0.578	0.23	0.71	0.06	–0.74	0.14		
18.7	2.52×10^{-2}	0.2392	0.4180	0.060	0.718	0.33	0.58	0.08	–0.82	0.14	–2.95	0.68
33.8	1.57×10^{-2}	0.4644	0.4398	0.125	1.029	0.45	0.43	0.12	–0.83	0.14	–2.49	0.30
51.7	9.01×10^{-3}	0.6090	0.4462	0.209	1.264	0.48	0.35	0.17	–0.94	0.14		
125.0	9.17×10^{-4}	0.9262	0.4375	0.829	2.193	0.42	0.20	0.38	–0.91	0.14		
278.0	7.77×10^{-6}	1.0542	0.5015	1.497	3.053	0.35	0.16	0.49	–1.08	0.14		

*Rate of Fe reduction, in percentage Fe(II) reduced per day, calculated from the first-order rate law: $[Fe(II)_{Tot}](t) = [Fe(II)_{Tot}]_{max}(1 - e^{-kt})$, where regression of the measured data produced $k = 0.1092$ ($R^2 = 0.863$) and 0.0312 ($R^2 = 0.971$) for the hematite and goethite experiments, respectively. Instantaneous reduction rates were determined from the first derivative of the first-order rate law: $d[Fe(II)_{Tot}]/dt = k[Fe(II)_{Tot}]_{max}(e^{-kt})$.

†$Fe(II)_{aq}$, $Fe(II)_{sorb}$ and $Fe(III)_{reac}$ concentrations calculated based on 3‰ fractionation between $Fe(III)_{reac}$ and $Fe(II)_{aq}$ (see text for details).

‡Fe_{reac} is the total reactive Fe pool, based on the components that were open to isotopic exchange: $Fe(II)_{aq} + Fe(II)_{sorb} + Fe(III)_{reac}$.

§X is the mole fraction of each component out of the total reactive Fe pool, calculated assuming a 3‰ fractionation between $Fe(III)_{reac}$ and $Fe(II)_{aq}$.

¶2σ errors were generated by the Excel add-in ISOPLOT (44), based on uncertainties in isotopic measurements and the fraction of Fe(II) in the HCl extractions. Values are not listed where uncertainties are ≥ 1‰.

Table 7 Reactive Fe species and calculated Fe isotope fractionations for *Geobacter sulfurreducens*

Day	Reduction rate % Fe(II)/d*	$Fe(II)_{aq}$ mM†	$Fe(II)_{sorb}$ mM	$Fe(III)_{reac}$ mM	Tot Reac Fe Pool mM‡	X-$Fe(II)_{aq}$§	X-$Fe(II)_{sorb}$	X-$Fe(III)_{reac}$	$\Delta Fe(II)_{aq} - Fe(II)_{sorb}$	2σ error¶	$\Delta Fe(II)_{aq} - Fe(III)_{reac}$	2σ error
Hematite experiment												
2.0	2.75×10^{-2}	0.041	0.077	0.240	0.358	0.11	0.22	0.67	–0.37	0.14	–3.13	0.19
4.0	2.51×10^{-2}	0.059	0.084	0.191	0.334	0.18	0.25	0.57	–0.53	0.14	–2.66	0.19
6.8	2.20×10^{-2}	0.163	0.169	0.381	0.713	0.23	0.24	0.53	–0.45	0.14	–3.31	0.28
12.7	1.68×10^{-2}	0.196	0.112	0.305	0.613	0.32	0.18	0.50	–0.37	0.14	–3.19	0.48
20.7	1.11×10^{-2}	0.233	0.148	0.363	0.744	0.31	0.20	0.49	–0.43	0.14	–2.86	0.20
35.8	5.83×10^{-3}	0.265	0.165	0.453	0.883	0.30	0.19	0.51	–0.43	0.14	–2.67	0.16
53.7	2.57×10^{-3}	0.372	0.188	0.467	1.027	0.36	0.18	0.45	–0.25	0.14	–3.98	0.57
126.7	9.08×10^{-5}	0.496	0.209	0.501	1.206	0.41	0.17	0.42	–0.47	0.14	–4.01	0.47
279.7	8.11×10^{-8}	0.472	0.213	0.385	1.070	0.44	0.20	0.36	–0.10	0.14	–3.57	0.40
Goethite experiment												
2.0	4.01×10^{-2}	0.015	0.177	0.025	0.217	0.07	0.82	0.11	–0.72	0.14		
4.0	3.83×10^{-2}	0.038	0.176	0.009	0.223	0.17	0.79	0.04	–0.71	0.14		
6.8	3.59×10^{-2}	0.113	0.437	0.008	0.558	0.20	0.78	0.01	–0.58	0.14	–3.89	0.92
12.7	3.14×10^{-2}	0.221	0.465	0.021	0.707	0.31	0.66	0.03	–0.70	0.14		
20.7	2.62×10^{-2}	0.326	0.508	0.061	0.895	0.36	0.57	0.07	–0.91	0.14		
35.8	1.85×10^{-2}	0.494	0.436	0.061	0.991	0.50	0.44	0.06	–0.72	0.14	–2.56	0.31
53.7	1.23×10^{-2}	0.654	0.419	0.250	1.323	0.49	0.32	0.19	–1.18	0.14		
126.7	2.33×10^{-3}	1.145	0.488	0.807	2.440	0.47	0.20	0.33	–1.02	0.14		
279.7	7.13×10^{-5}	1.366	0.632	1.249	3.247	0.42	0.19	0.38	–1.16	0.14		

*Rate of Fe reduction, in percentage Fe(II) reduced per day, calculated from the first-order rate law: $[Fe(II)_{Tot}](t) = [Fe(II)_{Tot}]_{max}(1 - e^{-kt})$, where regression of the measured data produced $k = 0.0458$ ($R^2 = 0.914$) and 0.0228 ($R^2 = 0.930$) for the hematite and goethite experiments, respectively. Instantaneous reduction rates were determined from the first derivative of the first-order rate law: $d[Fe(II)_{Tot}]/dt = k[Fe(II)_{Tot}]_{max}(e^{-kt})$.

†–¶See Table 6.

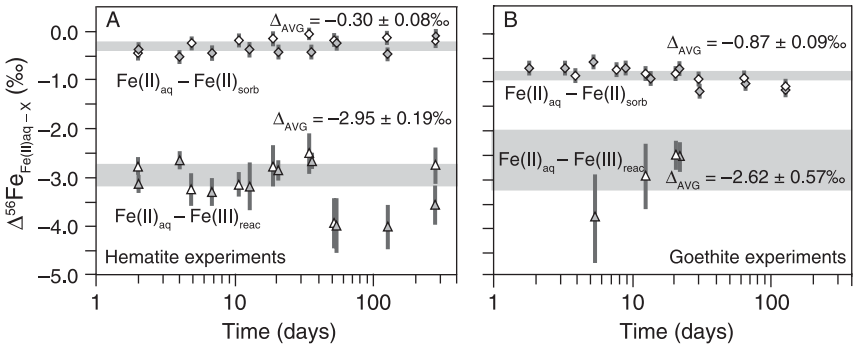

Fig. 7 Temporal variations in Fe(II)$_{aq}$ – Fe(II)$_{sorb}$ (diamonds) and Fe(II)$_{aq}$ – Fe(III)$_{reac}$ (triangles) isotope fractionation factors. White symbols show data from *Shewanella putrefaciens* experiments and grey symbols show data from *Geobacter sulfurreducens* experiments. Error bars for each time point reflect 2 σ uncertainties based on errors in measured δ^{56}Fe values for Fe(II)$_{aq}$ and Fe(II)$_{sorb}$, and calculated uncertainties in δ^{56}Fe values for Fe(III)$_{reac}$ based on uncertainties in the extrapolations shown in Fig. 6. Time points that had uncertainties in calculated values of δ^{56}Fe of reactive Fe(III) ≥ 1‰ are not included. Gray horizontal bars show weighted averages (Δ_{AVG}) for each fractionation factor, pooled for *S. putrefaciens* and *G. sulfurreducens* experiments. Data from Tables 6 and 7.

hematite and goethite substrates by *G. sulfurreducens* and *S. putrefaciens*. The $\Delta^{56}Fe_{Fe(II)aq-Fe(II)sorb}$ fractionations (Tables 6 and 7) are simply the difference between δ^{56}Fe values for Fe(II)$_{aq}$ and Fe(II)$_{sorb}$ recovered by NaAc extraction. The $\Delta^{56}Fe_{Fe(II)aq-Fe(III)reac}$ fractionations (Tables 6 and 7) are calculated using the δ^{56}Fe value measured for Fe(II)$_{aq}$ and the calculated $\delta^{56}Fe_{Fe(III)reac}$ values as described above. An important observation is that the $\Delta^{56}Fe_{Fe(II)aq-Fe(II)sorb}$ fractionations are functions of the oxide substrate and independent of bacterial species. Pooling the results for *G. sulfurreducens* and *S. putrefaciens*, the Fe(II)$_{aq}$ – Fe(II)$_{sorb}$ fractionation is –0.30 ± 0.08‰ for hematite and –0.87 ± 0.09‰ for goethite. These are identical within error to those determined by Crosby *et al.* (2005) using *G. sulfurreducens*. These fractionations appear to be consistent with time, within analytical error, despite wide changes in the amount of Fe(II)$_{aq}$ and Fe(II)$_{sorb}$ (Fig. 3), suggesting that these are equilibrium isotope fractionation factors. The consistently larger fractionation during sorption of Fe(II) to goethite compared to hematite could reflect differences in binding strengths between Fe(II) and the two oxide surfaces.

The $\Delta^{56}Fe_{Fe(II)aq-Fe(III)reac}$ fractionations are best constrained for experiments involving hematite because these contained the highest proportions of Fe(III) in the 0.5 M HCl extraction, allowing $\delta^{56}Fe_{Fe(III)reac}$ to be most precisely calculated from the mixing relations in Fig. 6. Pooling the results from the *G. sulfurreducens* and *S. putrefaciens* experiments with hematite produces a Fe(II)$_{aq}$ – Fe(III)$_{reac}$ fractionation of –2.95 ± 0.19‰, using the weighted-average approach employed in ISOPLOT, which weights data points by the inverse-square of their errors (Ludwig, 1991). Because the uncertainties in the calculated $\delta^{56}Fe_{Fe(III)reac}$ values are variable, depending on the proportion of Fe(III) in the 0.5 M HCl extraction, use of a weighted average in calculating isotopic fractionation factors is important so that fractionation factors for individual time points that have low errors are weighted more heavily in the average fractionation factor. Within the uncertainty of the $\Delta^{56}Fe_{Fe(II)aq-Fe(III)reac}$ fractionations for experiments using hematite, these fractionations appear to be the same for *G. sulfurreducens* and *S. putrefaciens* and do not systematically change with time within error (Fig. 7A).

The $\Delta^{56}Fe_{Fe(II)aq-Fe(III)reac}$ fractionations for experiments using goethite substrate are more poorly constrained than for hematite because of the greater uncertainty in calculating the $\delta^{56}Fe_{Fe(III)reac}$ values from the 0.5 M HCl extractions (Fig. 6). Based on our rejection of calculated $\delta^{56}Fe_{Fe(III)reac}$ values with an uncertainty ≥1‰ (discussed above), four $\Delta^{56}Fe_{Fe(II)aq-Fe(III)reac}$ fractionation factors may be calculated for the goethite experiments, producing a weighted average Fe(II)$_{aq}$ – Fe(III)$_{reac}$ fractionation of –2.62 ± 0.57‰. This value lies within error of that determined in the hematite experiments. These results suggest that the fundamental mechanism of Fe isotope fractionation during DIR of goethite and hematite by *G. sulfurreducens* and *S. putrefaciens* is the same.

The isotopic fractionation between Fe(II)$_{aq}$ and Fe(III)$_{reac}$ of –3.0‰ for the hematite experiments, consistent with the more poorly determined Fe(II)$_{aq}$ – Fe(III)$_{reac}$ fractionation in the goethite experiments within error, is essentially identical to that observed in abiological systems. The equilibrium fractionation between hexaquo-Fe(II) and hexaquo-Fe(III) in solution at 22 °C is –2.95 ± 0.38‰ (Welch *et al.*, 2003), and the equilibrium fractionation between aqueous Fe(III) and hematite at 98 °C is approximately –0.1‰ (Skulan *et al.*, 2002). The latter fractionation is believed to be similar at 22 °C, and combining the two fractionations gives an estimate of $\Delta^{56}Fe_{Fe(II)aq-hematite}$ of approximately –3.1‰. The similarity between this abiotic fractionation and the values for $\Delta^{56}Fe_{Fe(II)aq-Fe(III)reac}$ in our biological experiments is consistent with the inference that a reactive Fe(III) layer participates in isotope exchange during DIR. Moreover, the agreement of the $\Delta^{56}Fe_{Fe(II)aq-Fe(III)reac}$ fractionation measured in our experiments with that measured at equilibrium in abiological systems suggests that Fe isotope exchange in our experiments occurred under equilibrium conditions.

Proportions of $Fe(II)_{aq}$, $Fe(II)_{sorb}$, and $Fe(III)_{reac}$ in the reactive Fe pool

The relative proportions of $Fe(II)_{aq}$, $Fe(II)_{sorb}$, and $Fe(III)_{reac}$, combined with the $\Delta^{56}Fe_{Fe(II)aq-Fe(II)sorb}$ and $\Delta^{56}Fe_{Fe(II)aq-Fe(III)reac}$ fractionations, control the $\delta^{56}Fe$ values of these components, providing insight into the measured Fe isotope compositions in natural systems where DIR may be active. Crosby *et al.* (2005) defined the total reactive Fe pool as the mole sum of $Fe(II)_{aq}$ + $Fe(II)_{sorb}$ + $Fe(III)_{reac}$, which must *in toto* have the same Fe isotope composition as the oxide starting material ($\delta^{56}Fe_{Sys}$). The $Fe(II)_{aq}$ and $Fe(II)_{sorb}$ components are measured quantities based on the Fe concentration measurements and volume of the aqueous Fe(II) and the sum of Fe(II) that is extracted from the Na-acetate and HCl extractions. In contrast, the $Fe(III)_{reac}$ component cannot be easily measured because the only method to distinguish Fe(III) from the primary ferric oxide and the newly formed reactive ferric oxide is based on differences in isotopic composition. The isotopic composition of these different ferric iron pools are determined by analysis of the different extraction components and the starting ferric oxide composition. Based on isotopic mass balance constraints it is possible to calculate the molar fraction of $Fe(III)_{reac}$. Based on these mass balance constraints, the total reactive Fe pool, $M_{TotReacFe}$, is:

$$M_{TOT\ ReacFe} = [M_{Fe(II)aq}\delta^{56}Fe_{Fe(II)aq} + M_{Fe(II)sorb}\delta^{56}Fe_{Fe(II)sorb} - \delta^{56}Fe_{Fe(III)reac}(M_{Fe(II)aq} + M_{Fe(II)sorb})]/[\delta^{56}Fe_{Sys} - \delta^{56}Fe_{Fe(III)reac}] \quad (4)$$

Note that $M_{TotReacFe}$ in Equation 2 in Crosby *et al.* (2005) is incorrectly noted as $M_{Fe(III)reac}$. In order to make direct comparisons between the Fe isotope composition of $Fe(II)_{aq}$, $Fe(II)_{sorb}$, and $Fe(III)_{reac}$, it is necessary to normalize differences in the system Fe isotope composition. This is easily accomplished by normalizing the measured $\delta^{56}Fe$ values to $\delta^{56}Fe_{Sys} = 0$ to bring all data from the hematite and goethite experiments to a common reference. $M_{Fe(III)reac}$ is then calculated using the mass–balance relation:

$$\left[\frac{M_{Fe(II)aq}}{M_{Fe(II)aq} + M_{Fe(II)sorb} + M_{Fe(III)reac}}\right]\delta^{56}Fe_{Fe(II)aq} + \left[\frac{M_{Fe(II)sorb}}{M_{Fe(II)aq} + M_{Fe(II)sorb} + M_{Fe(III)reac}}\right]\delta^{56}Fe_{Fe(II)sorb} + \left[\frac{M_{Fe(III)reac}}{M_{Fe(II)aq} + M_{Fe(II)sorb} + M_{Fe(III)reac}}\right]\delta^{56}Fe_{Fe(III)reac} = 0 \quad (5)$$

which, when solved for $M_{Fe(III)reac}$, becomes:

$$M_{Fe(III)reac} = \frac{-\delta^{56}Fe_{Fe(II)aq}M_{Fe(II)aq} - \delta^{56}Fe_{Fe(II)sorb}M_{Fe(II)sorb}}{\delta^{56}Fe_{Fe(III)reac}} \quad (6)$$

It is important to note that $M_{Fe(III)reac}$ is not at all related to the amount of Fe(III) in the HCl extractions, but instead it is the moles of Fe(III) in the oxide substrate that are *required to attain isotopic mass balance* among $Fe(II)_{aq}$, $Fe(II)_{sorb}$, and $Fe(III)_{reac}$. Moreover, in calculating the $Fe(II)_{aq} - Fe(III)_{reac}$ fractionations, it is important that $M_{Fe(III)reac}$ is greater than the moles of Fe(III) in the HCl extractions so that none of the initial oxide is dissolved, and this condition was satisfied within the associated uncertainties in calculating $M_{Fe(III)reac}$. Note that the *intensive* variables ($\delta^{56}Fe$) do not need to be measured on the entire inventory of $Fe(II)_{aq}$, $Fe(II)_{sorb}$, and $Fe(III)_{reac}$ in the system. All parameters needed to calculate $M_{Fe(III)reac}$ in Equation 6 are measured quantities with the exception of $\delta^{56}Fe_{Fe(III)reac}$.

Crosby *et al.* (2005) noted that the proportions of $Fe(II)_{aq}$, $Fe(II)_{sorb}$, and $Fe(III)_{reac}$ changed during reduction, and that these changes were different for hematite and goethite using *G. sulfurreducens*. Some of the scatter in the temporal changes reported by Crosby *et al.* (2005) in $Fe(III)_{reac}$, particularly for goethite, likely reflect the generally greater uncertainty in $\delta^{56}Fe_{Fe(III)reac}$ for goethite and its affect on $M_{Fe(III)reac}$ in Equation 6. In this study therefore we use an alternative to Equation 6 by recasting in terms of the mean $\Delta^{56}Fe_{Fe(II)aq-Fe(III)reac}$ fractionation factor of 3‰ exemplified in Fig. 7. Substituting

$$\Delta^{56}Fe_{Fe(II)aq\text{-}Fe(III)reac} = \delta^{56}Fe_{Fe(II)aq} - \delta^{56}Fe_{Fe(III)reac} \quad (7)$$

or, re-arranged

$$\delta^{56}Fe_{Fe(III)reac} = \delta^{56}Fe_{Fe(II)aq} - \Delta^{56}Fe_{Fe(II)aq\text{-}Fe(III)reac} \quad (8)$$

into Equation 6 yields:

$$M_{Fe(III)reac} = \frac{-\delta^{56}Fe_{Fe(II)aq}M_{Fe(II)aq} - \delta^{56}Fe_{Fe(II)sorb}M_{Fe(II)sorb}}{\delta^{56}Fe_{Fe(II)aq} - \Delta^{56}Fe_{Fe(II)aq-Fe(III)reac}} \quad (9)$$

The advantage of this formulation for $M_{Fe(III)reac}$ is that it uses the average $\Delta^{56}Fe_{Fe(II)aq-Fe(III)reac}$ fractionation for the pooled dataset and so is not as sensitive to errors for individually calculated $\delta^{56}Fe_{Fe(III)reac}$ values for each sample. This in turn allows us to more accurately calculate the proportions of $Fe(II)_{aq}$, $Fe(II)_{sorb}$, and $Fe(III)_{reac}$ in the reactive Fe pools for all samples, including those that have large errors for $\delta^{56}Fe_{Fe(III)reac}$ that would otherwise be unusable. Using an average $\Delta^{56}Fe_{Fe(II)aq-Fe(III)reac}$ assumes that this fractionation applies to all samples, which, as discussed above, is supported by the results in Fig. 7.

The molar quantities of $Fe(II)_{aq}$, $Fe(II)_{sorb}$, and $Fe(III)_{reac}$, as well as the total size of the reactive Fe pool, are given in Table 6 for our new results using *S. putrefaciens* and hematite and goethite. These same quantities for our earlier results with *G. sulfurreducens*, recalculated using Equation 9, are given in

Table 7. The results suggest that the temporal changes in the reactive Fe components are strongly dependent on substrate but not on bacterial species. For hematite, the absolute abundance of $Fe(II)_{aq}$, $Fe(II)_{sorb}$, and $Fe(III)_{reac}$ increased modestly over time and then remained fairly constant toward the end of the experiment. For goethite, the total size of the reactive Fe pool, $Fe(II)_{aq}$, $Fe(II)_{sorb}$, and $Fe(III)_{reac}$ increased consistently over time (Tables 6 and 7). The maximum measured values for $Fe(III)_{reac}$ in the hematite and goethite systems (*c.* 0.4 and 1.0 mmol L^{-1}, respectively) were comparable to the total number of oxide surface sites present, based on the initial oxide mass loading (8.0 and 4.5 g L^{-1}, respectively), the measured oxide surface areas (*c.* 10 and 55 m^2 g^{-1}, respectively), and a standard mineral surface site density of *c.* 3.8 μmol sites m^{-2} (Davis & Kent, 1990). These results suggest that the $Fe(III)_{reac}$ pools detected here by dilute HCl extraction corresponded approximately to one surface layer of Fe(III) atoms. This is consistent with the conclusion of Crosby *et al.* (2005) that approximately one layer of Fe(III) atoms exchanged, based on the geometry of the oxide particles.

The relative proportions of $Fe(II)_{aq}$, $Fe(II)_{sorb}$, and $Fe(III)_{reac}$ in the reactive Fe pool are defined as $X_{Fe(II)aq}$, $X_{Fe(II)sorb}$, and $X_{Fe(III)reac}$, respectively, and are derived from Equation 9 using the relation:

$$X_i = \left[\frac{M_i}{M_{Fe(II)aq} + M_{Fe(II)sorb} + M_{Fe(III)reac}} \right] \quad (10)$$

We focus on the mole fractions of the reactive Fe pool to gain insight into the controls these components exert on the Fe isotope compositions. For hematite, a key observation is that $X_{Fe(III)reac}$ is initially the largest component of the reactive Fe pool and this monotonically decreases as $X_{Fe(II)aq}$ increases (Fig. 8A). $X_{Fe(II)sorb}$ remains essentially constant with time (Fig. 8A). For goethite, the largest changes in the relative proportions of reactive Fe species occurs for $X_{Fe(II)sorb}$, which initially is the major component, followed by a monotonic decrease with time for both bacterial species (Fig. 8B). In contrast to hematite, $X_{Fe(III)reac}$ for goethite begins as a small component, then decreases, followed by an increase with time. $X_{Fe(II)aq}$ monotonically increases up to ~30 days, followed by a slight decrease, where the inflection correlates with a rapid increase in $X_{Fe(III)reac}$ (Fig. 8B).

The contrasting behaviour of hematite and goethite in these experiments can only be partially explained in terms of existing knowledge of oxide surface chemistry. The greater surface area of goethite was almost certainly responsible for the higher initial extent of Fe(II) sorption (and corresponding high values for $X_{Fe(II)sorb}$) in this system, as well as the overall greater extent of enzymatic reduction (Roden & Zachara, 1996; Roden, 2006). There is, however, no obvious explanation for the contrasting evolution of the $Fe(III)_{reac}$ pool observed in the goethite and hematite systems. It is possible that the goethite surface may have been less susceptible than hematite to 'reworking' through surface reaction with Fe(II) (Coughlin & Stone, 1995), leading to a slower overall rate of destabilization of Fe(III) surface atoms and a slower increase in dilute HCl-extractable Fe(III) (i.e. $Fe(III)_{reac}$) toward a value approximating the surface site density for the mineral (see above). Detailed studies (e.g. X-ray absorption spectroscopy) of the structure of different Fe(III) oxide phases exposed to aqueous Fe(II) over extended periods of time will be required to address the appropriateness of this speculation. For the present purposes, we accept the calculated concentrations of $Fe(III)_{reac}$ and other components in the reactive Fe pool, and show how they affect the Fe isotope compositions that are produced by coupled Fe atom/electron transfer and Fe mass balance.

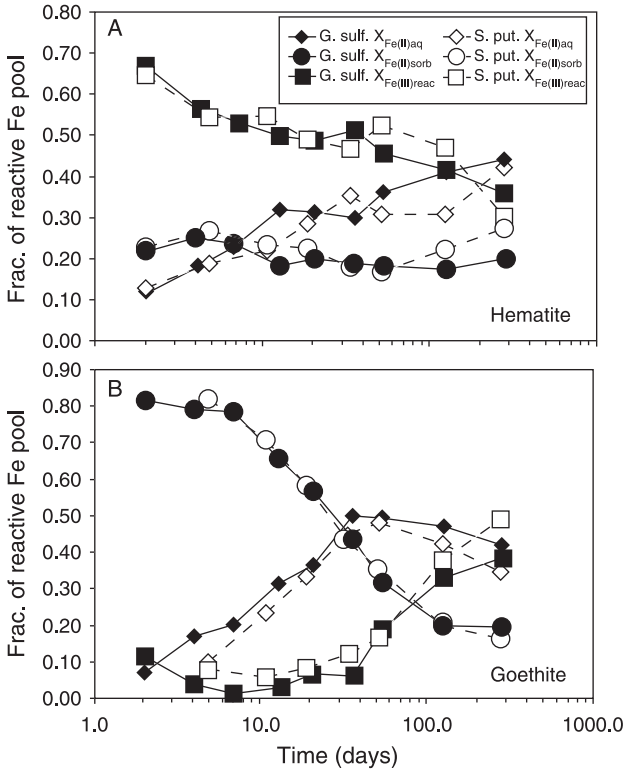

Fig. 8 Temporal variations in the proportions of $Fe(II)_{aq}$, $Fe(II)_{sorb}$, and $Fe(III)_{reac}$ in the reactive Fe pool, as calculated from equations 9 and 10. Changes in $X_{Fe(II)aq}$, $X_{Fe(II)sorb}$, and $X_{Fe(III)reac}$ with time are primarily a function of oxide substrate and independent of bacterial species. The changing proportions of $Fe(II)_{aq}$, $Fe(II)_{sorb}$, and $Fe(III)_{reac}$ will produce changes in the $\delta^{56}Fe$ values of these components. Data from Tables 6 and 7.

DISCUSSION

The new experiments on Fe isotope fractionations produced during reduction of hematite and goethite by *S. putrefaciens*, combined with the parallel experiments using *G. sulfurreducens* (Crosby *et al.*, 2005), allow us to develop a general model for Fe isotope fractionations produced during DIR for these substrates. Below we show that a key component to developing

a general model is the isotopic mass balance among $Fe(II)_{aq}$, $Fe(II)_{sorb}$, and $Fe(III)_{reac}$. In addition, we demonstrate that our model is consistent with Fe isotope variations observed in natural environments where DIR drives Fe cycling.

Electron transfer and atom exchange model of isotope fractionation

Evidence that interaction between $Fe(II)_{aq}$ and ferric oxides promotes dynamic surface rearrangements has been accumulating recently, although the first observations of these phenomena were made over two decades ago. Early studies reported electron transfer from sorbed Fe(II) to a spinel-like iron oxide material (Tronc *et al.*, 1984) and to ferrihydrite (Tronc *et al.*, 1992). Molecular orbital modelling showed that electron transfer could occur through overlapping d-orbitals of edge-sharing FeO_6 octahedra (Sherman, 1987). Rosso and co-workers have shown that charge transfer through a hematite lattice occurs via electron hopping at room temperature (Rosso *et al.*, 2003a; Kerisit & Rosso, 2006), and that electrons infused into the hematite surface during DIR can travel through the lattice to crystal defect sites (Rosso *et al.*, 2003b). Williams & Scherer (2004) used Mössbauer spectroscopy to observe exchange of ^{57}Fe and ^{56}Fe between aqueous Fe(II) and ferric oxide and hydroxide. They found that $^{57}Fe(II)$ sorption induces growth of an $^{57}Fe(III)$ layer that is similar (but not identical) to that of the underlying oxide, and similar results were found for ferrihydrite, goethite, and hematite. Silvester *et al.* (2005) confirmed these results, and concluded that electron transfer from sorbed $^{57}Fe(II)$ to the oxide surface was accompanied by growth of a new, ^{57}Fe-labelled ferric layer.

Using a slightly different strategy, Pedersen *et al.* (2005) radioactively labelled several ferric oxides with ^{55}Fe and measured ^{55}Fe release into solution upon addition of unlabelled aqueous Fe(II) to the system. They found that $^{55}Fe(II)$ was readily released into solution during Fe(II) sorption to ferrihydrite, lepidocrocite and goethite, although, in contrast to other results (Williams & Scherer, 2004; Crosby *et al.*, 2005), essentially no exchange was observed with hematite within the sensitivity limits of the experiment. For the systems where $^{55}Fe(II)$ was released into solution, the authors proposed that this was the result of Fe(II) – Fe(III) atom exchange at the oxide surface, followed by electron migration through the surface to radiolabelled Fe(III) atoms and subsequent dissolution of $^{55}Fe(II)$ (Pedersen *et al.*, 2005). This model can be applied to the data presented here, where the Fe isotope composition of the Fe(III) layer that forms at the oxide surface is distinct from that of the initial oxide. It is important to note that the ^{55}Fe experiments of Pedersen *et al.* (2005) only document the extent of isotopic exchange, not if attainment of isotopic equilibrium occurs among all Fe isotopes. In contrast, the results of our $\Delta^{56}Fe_{Fe(II)aq-Fe(III)reac}$ fractionation measurements document that at the reduction rates employed in the current experiments, isotopic equilibrium is likely. Electron transfer from sorbed Fe(II) to the oxide surface is shown as preceding Fe(II) – Fe(III) atom exchange in Fig. 1, although once Fe(II) is formed, these two steps could be reversed, as suggested in Pedersen *et al.* (2005).

We find that the same coupled electron transfer and atom exchange process controls Fe isotope fractionation during DIR by representative species of both Geobacteraceae and Shewanellaceae. We conclude that electron transfer from the cell to the ferric oxide or hydroxide surface produces aqueous Fe(II) that in turn promotes isotopic (atom) exchange with Fe(III) at the oxide or hydroxide surface. A critical observation is that the Fe isotope fractionation between $Fe(II)_{aq}$ and $Fe(III)_{reac}$ is identical to that measured in abiological systems, where the equilibrium Δ^{56}FeFe(II)aq – Fe(III)oxide/hydroxide fractionation is –3.1‰ at room temperature. The role of bacteria therefore appears to be to catalyse equilibrium Fe isotope exchange between these components through production of $Fe(II)_{aq}$ via electron transfer to the oxide substrate. It is important to note that the true Fe isotope fractionation factors involved in DIR are those among the reactive Fe pools $Fe(II)_{aq}$, $Fe(II)_{sorb}$, and $Fe(III)_{reac}$; it is *not* the apparent fractionation between $Fe(II)_{aq}$ and the *initial* ferric Fe oxide or hydroxide, a point stressed by Johnson *et al.* (2004), but one that is sometimes confused in the literature in discussions on comparing the Fe isotope fractionations of DIR to those of abiological systems.

The equilibrium $\Delta^{56}Fe_{Fe(II)aq-Fe(III)reac}$ fractionation is attained within days of the initiation of the reduction experiments (Fig. 7). This observation is also true for the $\Delta^{56}Fe_{Fe(II)aq-Fe(II)sorb}$ fractionation (Fig. 7), indicating that Fe isotope equilibrium is quickly established, and maintained, among all Fe components in the reactive Fe pool, at least under the conditions of our experiments. Although isotopic exchange between $Fe(II)_{aq}$ and $Fe(III)_{reac}$ probably occurs through the $Fe(II)_{sorb}$ species, if $Fe(II)_{aq}$ – $Fe(III)_{reac}$ and $Fe(II)_{aq}$ – $Fe(II)_{sorb}$ exchange occurs under equilibrium conditions, $Fe(II)_{sorb}$ – $Fe(III)_{reac}$ exchange must also occur under equilibrium conditions.

Williams & Scherer (2004) noted that Fe(III) sites in ferric oxide that had undergone isotopic exchange with $Fe(II)_{aq}$ were slightly distorted relative to ferric oxide that had not been exposed to $Fe(II)_{aq}$, and we speculate that such sites reflect those that have undergone $Fe(II)_{aq}$ – $Fe(III)_{reac}$ exchange in our experiments. Although for conceptual reasons we describe the $Fe(III)_{reac}$ component as a 'surface layer', it is entirely possible that this component is non-uniformly distributed on the oxide surface and may in fact represent defects. In addition, delivery of electrons by Fe(III)-reducing bacteria to the surface may occur at sites different than those undergoing isotopic exchange to the degree that transport of electrons may occur on or at the mineral surface. We suggest, however, that the Fe(III) atoms that serve as the terminal electron acceptor are those that participate in isotopic exchange with Fe(III).

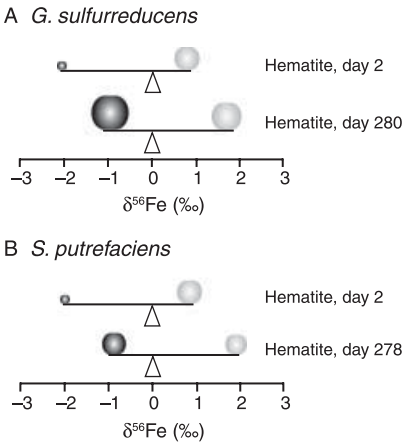

Fig. 9 Diagrammatic illustration of isotopic mass balance relations between $Fe(II)_{aq}$ and $Fe(III)_{reac}$ in the hematite experiments. Black and grey circles show relative amounts of $Fe(II)_{aq}$ and $Fe(III)_{reac}$, respectively. The $\delta^{56}Fe$ scale is normalized to a starting composition of the hematite substrate of zero, represented by the triangular fulcrums. The beams of each balance are 3‰ long, representing the average fractionation between $Fe(II)_{aq}$ and $Fe(III)_{reac}$. Although the $Fe(II)_{aq}$ – $Fe(III)_{reac}$ fractionation is constant over time (Fig. 7), the changing proportions of $Fe(II)_{aq}$ and $Fe(III)_{reac}$ in the total reactive Fe pool (Fig. 8) will produce changes in the $\delta^{56}Fe$ values of these components. The same mass-balance principles apply to the goethite experiments. $Fe(II)_{sorb}$ is omitted for clarity.

Fe isotope signatures of DIR: the critical role of mass balance

The changes in $\delta^{56}Fe$ values of $Fe(II)_{aq}$ and $Fe(II)_{sorb}$ that accompany DIR (Fig. 5) are determined by the isotopic mass balance constraints of the $Fe(III)_{reac}$ component. Although many studies have now shown that DIR produces low-$\delta^{56}Fe$ $Fe(II)_{aq}$ (Beard *et al.*, 1999, 2003a; Icopini *et al.*, 2004; Johnson *et al.*, 2005), this work and our previous results (Crosby *et al.*, 2005) are the first to measure the required high-$\delta^{56}Fe$ component. If DIR catalyses equilibrium isotope partitioning between aqueous Fe(II) and 'new' Fe(III) oxide material at the substrate surface through coupled electron transfer and atom exchange for both hematite and goethite, this process seems likely to be applicable to other oxides.

The actual $\delta^{56}Fe$ values of $Fe(II)_{aq}$ and $Fe(III)_{reac}$ at any given time will depend on the relative sizes of the reactive Fe pools. This is illustrated schematically in Fig. 9, which shows a series of balances, in which the fulcrum is the starting isotopic composition of the oxide ($\delta^{56}Fe$ of the system; normalized to 0‰ for convenience), and the length of the beam represents the –3.0‰ fractionation measured between $Fe(II)_{aq}$ and $Fe(III)_{reac}$. The black and grey circles represent the relative amounts of $Fe(II)_{aq}$ and $Fe(III)_{reac}$, respectively. For example, after 2 days of hematite reduction by *G. sulfurreducens*, $X_{Fe(II)aq}$ is much smaller than $X_{Fe(III)reac}$ (Fig. 8A). Therefore $Fe(II)_{aq}$ is shifted to lower $\delta^{56}Fe$ values to balance out the larger pool of $Fe(III)_{reac}$. This would imply that during the initial stages of DIR, the largest pool of 'mobilized Fe' (e.g. that open to atom exchange) actually lies in reactive surface Fe(III) sites in the oxide and not in Fe(II), as might be generally expected for DIR. At the end of the experiment (day 280), $X_{Fe(II)aq}$ has increased dramatically due to overall Fe(III) reduction, producing a decrease in $X_{Fe(III)reac}$ (Fig. 8A), which in turn requires a shift in the Fe isotope composition of $Fe(II)_{aq}$ to higher $\delta^{56}Fe$ values. The same relations are shown for the beginning and end of the *S. putrefaciens* experiments with hematite. Similar mass–balance relations would exist for the goethite experiments. For simplicity, we do not include $Fe(II)_{sorb}$ in Fig. 9, but we will explicitly account for $Fe(II)_{sorb}$ below. The very high proportion of $Fe(II)_{sorb}$ in the initial stages of DIR using goethite (Fig. 8B) indicates that sorbed Fe(II) becomes more significant in terms of molar balance in the reactive Fe pool; this would be represented as a third 'balance point' on the lever in Fig. 9. $Fe(II)_{sorb}$ becomes less important at later time periods for the goethite experiments (Fig. 8B), where the $\delta^{56}Fe$ values should be largely controlled by the relative proportions of $Fe(II)_{aq}$ and $Fe(III)_{reac}$.

The model illustrated in Fig. 9 is a simple two-component mixing model that predicts an inverse correlation between $X_{Fe(III)reac}$ and $\delta^{56}Fe_{Fe(II)aq}$ via the relation:

$$\delta^{56}Fe_{Fe(II)aq} = \Delta^{56}Fe_{Fe(II)aq-Fe(III)reac}\, X_{Fe(III)reac} \qquad (11)$$

where the $\delta^{56}Fe$ value for the initial oxide is normalized to zero and $\Delta^{56}Fe_{Fe(II)aq-Fe(III)reac} = -3.0‰$. Such a relation is generally observed in our experiments (Fig. 10), with the exception that the data for the hematite and goethite experiments lie at slightly lower $\delta^{56}Fe_{Fe(II)aq}$ values at intermediate $X_{Fe(III)reac}$, and at $X_{Fe(III)reac} \leq \sim 0.2$, the $\delta^{56}Fe_{Fe(II)aq}$ values for the goethite experiments lie significantly below a simple mixing line. These differences are well explained when the effects of $Fe(II)_{sorb}$ are explicitly calculated. A predicted relation between $X_{Fe(III)reac}$ and $\delta^{56}Fe_{Fe(II)aq}$ that accounts for $Fe(II)_{sorb}$ may be obtained using Equation 9, the average $\Delta^{56}Fe_{Fe(II)aq-Fe(III)reac}$ and $\Delta^{56}Fe_{Fe(II)aq-Fe(II)sorb}$ fractionations from Fig. 7, the relation between $M_{Fe(II)aq}$ and $M_{Fe(II)sorb}$ from Fig. 4, and regression of the observed relations between $M_{Fe(III)reac}$ and $M_{Fe(II)aq}$ (see caption, Fig. 10). In the case of the hematite experiments, the relatively small proportion of $X_{Fe(II)sorb}$ (Fig. 8A) and small $\Delta^{56}Fe_{Fe(II)aq-Fe(II)sorb}$ fractionation factor produces a shift in $\delta^{56}Fe_{Fe(II)aq}$ values <0.05‰ relative to the simple two-component mixing line of Equation 11 (Fig. 10), which is insignificant. For the goethite experiments, the shift in $\delta^{56}Fe_{Fe(II)aq}$ that is due to sorption is largest at low $X_{Fe(III)reac}$, and this shift is well modelled using Equation 9 (Fig. 10). At $X_{Fe(III)reac} = 0.1$, the simple two-component mixing model of Equation 11 predicts $\delta^{56}Fe_{Fe(II)aq} = -0.30‰$, and the sorption model of Equation 9 predicts $\delta^{56}Fe_{Fe(II)aq} = -0.68‰$, indicating that the shift due to sorption is 0.38‰. At $X_{Fe(III)reac} = 0.3$, the simple mixing model predicts $\delta^{56}Fe_{Fe(II)aq} = -0.90‰$, whereas the sorption model predicts $\delta^{56}Fe_{Fe(II)aq} = -1.07‰$, indicating a shift due to

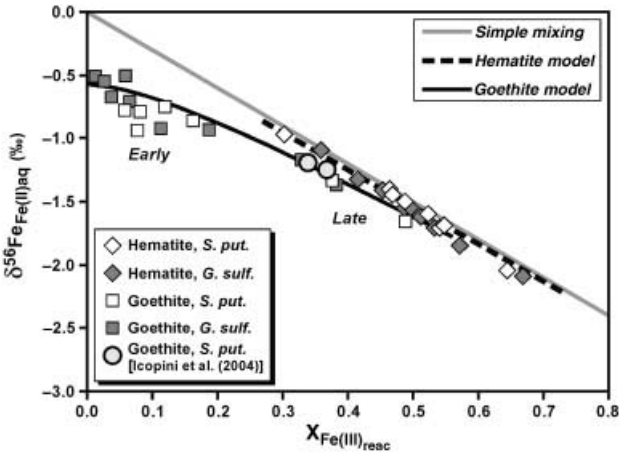

Fig. 10 Variations between $\delta^{56}Fe_{Fe(II)aq}$ and $X_{Fe(III)reac}$ for *Shewanella putrefaciens* and *Geobacter sulfurreducens* DIR experiments from this study and that of Icopini *et al*. (2004). The negative correlation between $\delta^{56}Fe_{Fe(II)aq}$ and $X_{Fe(III)reac}$ is predicted by a simple two-component mixing model (solid grey line) such as the mass-balance model illustrated in Fig. 9 (Equation 11). Deviations from a simple mixing relation occur due to the effects of $Fe(II)_{sorb}$, and model curves that account for sorption are shown for hematite (dashed black line) and goethite (solid black line) based on equations 9 and 10. The effect of sorption on the $\delta^{56}Fe_{Fe(II)aq}$ values is very small for hematite (<0.05‰), but is more significant for goethite. At $X_{Fe(III)reac} = 0.1$, a value that was typical early in the goethite experiments, the effect of sorption on $\delta^{56}Fe_{Fe(II)aq}$ was ~0.3–0.5‰ relative to a simple mixing model, and this effect decreased to ~0.1‰ later in the experiments as $X_{Fe(III)reac}$ increased (see also Fig. 8). The proportion of $Fe(II)_{sorb}$ was low relative to $Fe(II)_{aq}$ for the experiments of Icopini *et al*. (2004), which produces a moderate $X_{Fe(III)reac}$ of ~0.3–0.4 and a small isotopic effect from sorption of <0.2‰. $\delta^{56}Fe$ values normalized to zero for the 'system' (initial oxide) to allow comparison of different experiments. Model curves used the following regressions from the experiments. Hematite: $M_{Fe(III)reac} = 0.524\ M_{Fe(II)aq} + 0.231$ ($R^2 = 0.682$). Goethite: $M_{Fe(III)reac} = 3153\ (1 - e^{-0.01223\ [M_{Fe(II)aq}]}) - 725(1 - e^{-0.0537\ [M_{Fe(II)aq}]})$ ($R^2 = 0.996$).

sorption of only 0.17‰. The effect of Fe(II) sorption in the goethite experiments is only significant at low $X_{Fe(III)reac}$, which occurs during the initial stages of reduction (<1%), and sorption becomes insignificant in determining the $\delta^{56}Fe$ values for $Fe(II)_{aq}$ toward the end of the experiment, where $X_{Fe(III)reac} > 0.3$ and the extent of reduction is >2–3%. It is important to note that because $Fe(II)_{sorb}$ is only one of the components in the reactive Fe pool, the Fe isotope effects of sorption will always be less than the measured $Fe(II)_{aq}$ – $Fe(II)_{sorb}$ fractionation factor.

Comparison with previous studies

The most directly comparable study of Fe isotope fractionation during DIR is that of Icopini *et al.* (2004), who investigated reduction of goethite by *S. putrefaciens* in the presence and absence of the electron shuttling analogue AQDS. Although Icopini *et al.* (2004) did not measure the Fe isotope compositions of $Fe(II)_{sorb}$, they report $Fe(II)_{aq}$ and $Fe(II)_{sorb}$ concentrations and $\delta^{56}Fe_{Fe(II)aq}$, allowing us to plot their results in Fig. 10 using the $\Delta^{56}Fe_{Fe(II)aq-Fe(II)sorb}$ fractionation factor determined for goethite. In contrast to the proposal by Icopini *et al.* (2004) that sorption of Fe(II) was the major factor in producing low-$\delta^{56}Fe$ values for $Fe(II)_{aq}$, their experiments plot between $X_{Fe(III)reac} = 0.3 - 0.4$, where the effect of Fe(II) sorption on goethite is less than 0.1‰ (Fig. 10). We conclude therefore that sorption of Fe(II) had essentially no effect on the $\delta^{56}Fe$ values for $Fe(II)_{aq}$ in the DIR experiments of Icopini *et al.* (2004). These contrasting conclusions demonstrate the importance of a detailed *direct* assessment of the Fe isotope mass balance when inferring the mechanisms of Fe isotope fractionation.

Additional studies of Fe isotope fractionation during DIR cannot be explicitly plotted in Fig. 10 because they did not always include measurements of $Fe(II)_{sorb}$ concentrations, and in the case of experiments that involved ferrihydrite, the $\Delta^{56}Fe_{Fe(II)aq-Fe(II)sorb}$ fractionation factor is unknown. In the study of hematite reduction by *S. alga* by Beard *et al.* (2003a), however, it seems likely that sorption did not exert a significant effect on the $\delta^{56}Fe$ values for $Fe(II)_{aq}$, given the small $\Delta^{56}Fe_{Fe(II)aq-Fe(II)sorb}$ fractionation we measure for hematite and the likely small inventory of $Fe(II)_{sorb}$ in those experiments. The DIR experiments that have used ferrihydrite and *S. alga* and *G. sulfurreducens* by Johnson *et al.* (2005) produced relatively large inventories of $Fe(II)_{sorb}$. Johnson *et al.* (2005) interpreted temporal changes in $\delta^{56}Fe_{Fe(II)aq}$ during the first 21 days of longer-term experiments (their experiments 2 and 3), prior to formation of well-crystallized Fe(II) products, to reflect kinetic effects due to rapid sorption as a function of Fe reduction rates. In light of the current study, however, the changes in $\delta^{56}Fe_{Fe(II)aq}$ values observed by Johnson *et al.* (2005) could also reflect temporal changes in $X_{Fe(III)reac}$ rather than a kinetic effect associated with high rates of Fe(III) reduction and concomitant Fe(II) sorption. Rigorous calculation of the relations between $\delta^{56}Fe_{Fe(II)aq}$ and $X_{Fe(III)reac}$ for the studies of Johnson *et al.* (2005) will require knowledge of the $\Delta^{56}Fe_{Fe(II)aq-Fe(II)sorb}$ fractionation factor for ferrihydrite, which at present is unknown.

Fe isotope signatures of DIR in natural environments

Iron isotope data for $Fe(II)_{aq}$ in pore fluids from suboxic modern marine sediments where Fe cycling is driven by DIR allow us to test the isotopic mass balance relations predicted by our experimental results. Data from nonsulfidic sediment sections of the Monterey Canyon and Santa Barbara basin (California margin; Severmann *et al.*, 2006) and the Amazon-Guiana shelf (NE South American margin; Bergquist & Boyle, 2006) fall along a rough trend of increasing $\delta^{56}Fe$ values for porewater $Fe(II)_{aq}$ contents (Fig. 11). Using a simple two-component mixing line (Equation 11), low $Fe(II)_{aq}$ contents will be associated with high $X_{Fe(III)reac}$, which in turn will produce low $\delta^{56}Fe_{Fe(II)aq}$ values, and such relations are generally observed in Fig. 11. Moreover, the range in $\delta^{56}Fe_{Fe(II)aq}$ values measured for the pore fluids matches that obtained in our experiments.

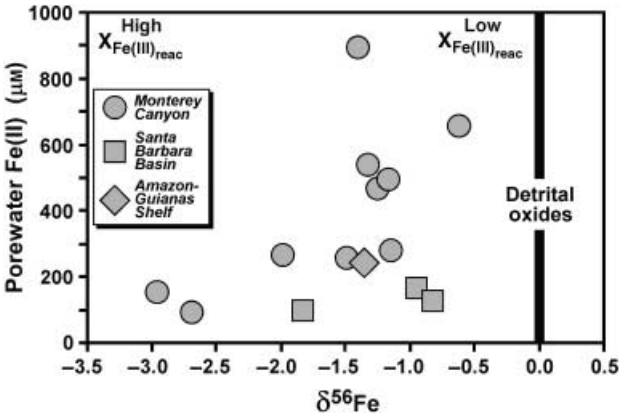

Fig. 11 Isotopic-concentration variations for pore fluids from low-sulfide samples of modern marine sediments where DIR is interpreted to drive Fe cycling. The initial ferric oxides are inferred to have had δ^{56}Fe values near zero, the average of detrital oxides (Beard *et al*., 2003b). The lowest measured δ^{56}Fe values for pore fluid $Fe(II)_{aq}$ reaches the theoretically lower limit of –3.0‰ for DIR in a single step of reduction, and the mass-balance relations between $Fe(II)_{aq}$ and $Fe(III)_{reac}$ (Fig. 10) predict that such low δ^{56}Fe values should occur in pore fluids that have very low $Fe(II)_{aq}$ contents. Such compositions would be inferred to be in equilibrium with ferric oxides that had a high proportion of $Fe(III)_{reac}$; note that $Fe(III)_{reac}$, as defined in this study, is not equal to the total inventory of 'reactive Fe(III)' as commonly defined in sediment studies, but is the reactive surface layer that undergoes isotopic exchange with $Fe(II)_{aq}$. Pore fluids that have higher δ^{56}Fe values should have higher $Fe(II)_{aq}$ contents, which are predicted to reflect exchange with a relatively small pool of $Fe(III)_{reac}$. The measured isotopic-concentration variations in nature generally follow the mass-balance relations predicted from Fig. 10. Data for the Monterey Canyon and Santa Barbara basin from Severmann *et al*. (2006). The datum from the Amazon-Guianas shelf is from Bergquist & Boyle (2006).

Assuming an initial δ^{56}Fe value for ferric oxide of zero, the theoretical lower limit for $\delta^{56}Fe_{Fe(II)aq}$ produced by DIR in a single batch experiment is –3.0‰ when $X_{Fe(III)reac}$ approaches unity (Equation 11). The upper limit for $\delta^{56}Fe_{Fe(II)aq}$ will depend on the minimum threshold for $X_{Fe(III)reac}$ (Fig. 10), and in the case of goethite, a small effect due to $Fe(II)_{sorb}$; in the case of our DIR experiments, the maximum $\delta^{56}Fe_{Fe(II)aq}$ value was approximately –0.5‰, and this is similar to the maximum value observed in the pore fluids from the California margin sediments that contained relatively low sulfide contents. In all cases, however, the δ^{56}Fe values for $Fe(II)_{aq}$ produced by DIR should be lower than the δ^{56}Fe value for the initial ferric oxides, which in nature, should initially have had δ^{56}Fe values of approximately zero if they were detrital (Beard *et al.*, 2003b). The scatter in the $Fe(II)_{aq} - \delta^{56}$Fe relations in the natural pore fluids (Fig. 11) likely reflects complexities imposed by the open nature of the system in terms of fluid flow, and uncertainties in the amount of $Fe(II)_{sorb}$. Nevertheless, these data from natural systems confirm that low-δ^{56}Fe values for $Fe(II)_{aq}$ may represent a general 'fingerprint' for DIR, and to a first approximation the absolute δ^{56}Fe values for $Fe(II)_{aq}$ are likely to reflect the relative abundance of aqueous Fe(II) and reactive Fe(III) pools that are open to isotopic exchange.

CONCLUSIONS

Iron isotope fractionations produced during reduction of hematite and goethite by *G. sulfurreducens* and *S. putrefaciens* that were grown under identical conditions are similar, suggesting a common mechanism. Aqueous Fe(II) that has low δ^{56}Fe values has been a ubiquitous observation in previous Fe isotope studies of DIR, and this is now understood to be produced by coupled electron and atom exchange between $Fe(II)_{aq}$ and reactive Fe(III) on the ferric oxide or hydroxide surface (defined as $Fe(III)_{reac}$). The Fe isotope fractionation between $Fe(II)_{aq}$ and $Fe(III)_{reac}$, defined as $\Delta^{56}Fe_{Fe(II)aq-Fe(III)reac}$, is well constrained at –2.95 ± 0.19‰ for experiments using *G. sulfurreducens* and *S. putrefaciens* and hematite as the substrate, and this is identical within error to the –3.1‰ equilibrium fractionation determined between $Fe(II)_{aq}$ and ferric oxide or hydroxide in abiological systems at room temperature. The $\Delta^{56}Fe_{Fe(II)aq-Fe(III)reac}$ fractionation factor for *G. sulfurreducens* and *S. putrefaciens* using goethite as the substrate is less well constrained because of greater carry over of sorbed Fe(II) during sequential acid stripping, but lies within error of the isotopic fractionation determined using hematite as the substrate. We therefore suggest that the mechanism that produces Fe isotope fractionation during DIR is the same regardless of substrate or species, at least to a first approximation.

Although the δ^{56}Fe values for $Fe(II)_{aq}$ produced during DIR are always negative, they may vary from approximately –3.0‰ to approximately –1.0‰, dependent on the relative proportions of the Fe reservoirs $Fe(II)_{aq}$, $Fe(II)_{sorb}$, and $Fe(III)_{reac}$ that are open to isotopic exchange during reduction. The temporal changes in the proportions of these species were distinct for the two substrates but identical for both *G. sulfurreducens* and *S. putrefaciens* for a given substrate. In our experiments, the isotopic effects of $Fe(II)_{sorb}$ are insignificant for reduction of hematite due to the relatively low quantities of $Fe(II)_{sorb}$ and the small $\Delta^{56}Fe_{Fe(II)aq-Fe(II)sorb}$ fractionation factor of –0.30 ± 0.08‰ for hematite. The δ^{56}Fe values for $Fe(II)_{aq}$ during DIR of hematite are therefore well approximated by a simple two-component mixing relation, where high proportions of $Fe(III)_{reac}$ are balanced by low $Fe(II)_{aq}$ contents that have low-$\delta^{56}Fe_{Fe(II)aq}$ values, and low proportions of $Fe(III)_{reac}$ are balanced by higher $Fe(II)_{aq}$ contents that have less negative $\delta^{56}Fe_{Fe(II)aq}$ values. Although natural hematite may have higher surface areas than that used in our experiments (~10 $m^2\ g^{-1}$), the small $\Delta^{56}Fe_{Fe(II)aq-Fe(II)sorb}$ fractionation factor for hematite indicates that the isotopic effects of sorption are likely to be insignificant for all sizes of hematite.

The relatively large surface area of the goethite used in the experiments (~55 $m^2\ g^{-1}$) increased the proportion of $Fe(II)_{sorb}$ during the early stages of DIR; coupled with the larger magnitude of the $\Delta^{56}Fe_{Fe(II)aq-Fe(II)sorb}$ fractionation factor of –0.87 ± 0.09‰ for goethite, the isotopic effects of $Fe(II)_{sorb}$ during the initial stages of DIR were more significant

for goethite than for hematite. At less than 1% reduction of goethite, Fe(II) sorption decreases the δ^{56}Fe values for $Fe(II)_{aq}$ by 0.3–0.4‰ relative to that which would be produced in a simple two-component $Fe(II)_{aq}$ – $Fe(III)_{reac}$ exchange model. At higher extents of reduction, >2–3%, the effect of Fe(II) sorption on the δ^{56}Fe values for $Fe(II)_{aq}$ decreases to 0.2‰ or less.

The current experiments were designed so that very slow rates of Fe(III) reduction were attained to maximize the likelihood of maintaining isotopic equilibrium. Even at the relatively high rates of initial Fe(III) reduction, however, Fe isotope equilibrium appears to have been established among $Fe(II)_{aq}$, $Fe(II)_{sorb}$, and $Fe(III)_{reac}$ within a few days, suggesting that in DIR systems that undergo greater rates or extents of reduction, an equilibrium isotope fractionation model may be applicable. It seems likely that the maximum size of the $Fe(III)_{reac}$ pool will be equal to a monolayer of surface sites because isotopic exchange rates should markedly decrease if Fe atoms are involved that occur deeper in the oxide. We therefore envision that at greater extents of reduction in a closed system, the proportion of $Fe(II)_{aq}$ will increase relative to a fixed maximum pool of $Fe(III)_{reac}$, requiring a decreasingly negative $\delta^{56}Fe_{Fe(II)aq}$ value. The $Fe(II)_{aq}$ concentration–$\delta^{56}Fe_{Fe(II)aq}$ relations that are predicted by our $Fe(II)_{aq}$ – $Fe(II)_{sorb}$ – $Fe(III)_{reac}$ mass balance model for DIR are similar to those observed in pore fluids from modern marine sediments where DIR drives Fe cycling. Assuming that the initial oxide has a δ^{56}Fe value equal to zero, the δ^{56}Fe value of $Fe(II)_{aq}$ will approach zero in the last stages of reduction as the final $Fe(III)_{reac}$ pool approaches the limit of $\delta^{56}Fe = +3‰$, as required by the $Fe(II)_{aq}$ – $Fe(III)_{reac}$ fractionation factor. It is important to note, however, that in an open system where porewater $Fe(II)_{aq}$ is lost, a situation that is commonly observed in natural DIR systems, the δ^{56}Fe values for $Fe(II)_{aq}$ will be maintained at relatively negative values to greater extents of reduction, to the degree that the size of the $Fe(II)_{aq}$ pool remains small; in such a case, the $\delta^{56}Fe_{Fe(II)aq}$ values would eventually become positive, but only during the last stages of reduction.

Ancient sedimentary rock sequences that contain substantial inventories of Fe(II)-bearing authigenic minerals such as siderite ($FeCO_3$) and magnetite (Fe_3O_4), prominent in banded iron formations, are likely to represent ideal settings to search for an Fe isotope fingerprint of DIR in the ancient rock record. Such fingerprints allow testing of proposals that DIR may have produced the large inventories of these minerals (Konhauser *et al.*, 2005). Calculation of the δ^{56}Fe values for ancient $Fe(II)_{aq}$ from measurement of authigenic minerals such as siderite and magnetite is possible using recent determinations of the $Fe(II)_{aq}$-siderite and $Fe(II)_{aq}$-magnetite Fe isotope fractionation factors (Wiesli *et al.*, 2004; Johnson *et al.*, 2005), allowing us to connect the Fe isotope fractionations measured in DIR experiments with the rock record. Ultimately, such an approach is likely to constrain when DIR developed as a significant metabolism on Earth.

ACKNOWLEDGEMENTS

G. Scott at the University of Alabama is gratefully acknowledged for assistance with experimental sampling and data collection. TEM work was performed by Dr H. Xu at the University of Wisconsin-Madison Materials Science Center, and XRD analyses were done at the WISC Nanogeoscience lab. Constructive criticism by three anonymous reviewers and the Associate Editor, Dianne Newman, are greatly appreciated. Funding was provided by NSF grant EAR-0525417 to C.M.J., B.L.B., and E.E.R., and an NSF predoctoral fellowship to H.A.C.

REFERENCES

Amonette J, Workman D, Kennedy D, Fruchter J, Gorby Y (2000) Dechlorination of carbon tetrachloride by Fe(II) associated with goethite. *Environmental Science and Technology* **34**, 4606–4613.

Archer C, Vance D (2006) Coupled Fe and S isotope evidence for Archean microbial Fe(III) and sulfate reduction. *Geology* **34**, 153–156.

Beard B, Johnson C, Cox L, Sun H, Nealson K, Aguilar C (1999) Iron isotope biosignatures. *Science* **285**, 1889–1892.

Beard B, Johnson C, Skulan J, Nealson K, Cox L, Sun H (2003a) Application of Fe isotopes to tracing the geochemical and biological cycling of Fe. *Chemical Geology* **195**, 87–117.

Beard B, Johnson C, Von Damm K, Poulson R (2003b) Iron isotope constraints on Fe cycling and mass balance in oxygenated Earth oceans. *Geology* **31**, 629–632.

Bergquist BA, Boyle EA (2006) Iron isotopes in the Amazon River system: weathering and transport signatures. *Earth and Planetary Science Letters* **248**, 54–68.

Buerge I, Hug S (1999) Influence of mineral surfaces on chromium(VI) reduction by Iron(II). *Environmental Science and Technology* **33**, 4285–4291.

Caccavo F, Blakemore R, Lovley D (1992) A hydrogen-oxidizing, Fe(III)-reducing microorganism from the Great Bay Estuary, New Hampshire. *Applied and Environmental Microbiology* **58**, 3211–3216.

Childers S, Ciufo S, Lovley D (2002) Geobacter metallireducens accesses insoluble Fe(III) oxide by chemotaxis. *Nature* **416**, 767–769.

Coughlin B, Stone A (1995) Nonreversible adsorption of divalent metal ions (Mn-II, Co-II, Ni-II, Cu-II, and Pb-II) onto goethite: effects of acidification, Fe-II addition, and picolinic acid additon. *Environmental Science & Technology* **29**, 2445–2455.

Crosby H, Johnson C, Roden E, Beard B (2005) Coupled Fe(II) – Fe(III) electron and atom exchange as a mechanism for Fe isotope fractionation during dissimilatory iron oxide reduction. *Environmental Science and Technology* **39**, 6698–6704.

Davis JA, Kent DB (1990) Surface Complexation Modeling in Aqueous Geochemistry. *Reviews in Mineralogy* **23**, 177–260.

Elsner M, Schwarzenbach R, Haderlein S (2004) Reactivity of Fe(II)-bearing minerals toward reductive transformation of organic contaminants. *Environmental Science and Technology* **38**, 799–807.

Fredrickson J, Zachara J, Kennedy D, Dong H, Onstott T, Hinman N, Li S (1998) Blogenic iron mineralization accompanying the dissimilatory reduction of hydrous ferric oxide by a groundwater bacterium. *Geochimica et Cosmochimica Acta* **62**, 3239–3257.

Fredrickson J, Zachara J, Balkwill D, Kennedy D, Li S, Kostandarithes H, Daly M, Romine M, Brockman F (2004) Geomicrobiology of high-level nuclear waste-contaminated vadose sediments at the Hanford Site, Washington State. *Applied and Environmental Microbiology* **70**, 4230–4241.

Gorby Y, Yanina S *et al.* (2006) Electrically conductive bacterial nanowires produced by *Shewanella oneidensis* strain MR-1 and other microorganisms. *Proceedings of the National Academy of Sciences of the USA* **103**, 11 358–11 363.

Hansel C, Benner S, Nico P, Fendorf S (2004) Structural constraints of ferric (hydr) oxides on dissimilatory iron reduction and the fate of Fe(II). *Geochimica et Cosmochimica Acta* **68**, 3217–3229.

Icopini G, Anbar A, Ruebush S, Tien M, Brantley S (2004) Iron isotope fractionation during microbial reduction of iron: the importance of adsorption. *Geology* **32**, 205–208.

Johnson C, Beard B (2006) Fe isotopes: an emerging technique for understanding modern and ancient biogeochemical cycles. *GSA Today* **16**, 4–10.

Johnson C, Beard B, Roden E, Newman D, Nealson K (2004) Isotopic constraints on biogeochemical cycling of Fe. *Geochemistry of Non-Traditional Stable Isotopes* **55**, 359–408.

Johnson C, Roden E, Welch S, Beard B (2005) Experimental constraints on Fe isotope fractionation during magnetite and Fe carbonate formation coupled to dissimilatory hydrous ferric oxide reduction. *Geochimica et Cosmochimica Acta* **69**, 963–993.

Kerisit S, Rosso K (2006) Computer simulation of electron transfer at hematite surfaces. *Geochimica et Cosmochimica Acta* **70**, 1888–1903.

Konhauser K, Newman D, Kappler A (2005) The potential significance of microbial Fe(III) reduction during deposition of Precambrian banded iron formations. *Geobiology* **3**, 167–177.

Kukkadapu R, Zachara J, Smith S, Fredrickson J, Liu C (2001) Dissimilatory bacterial reduction of Al-substituted goethite in subsurface sediments. *Geochimica et Cosmochimica Acta* **65**, 2913–2924.

Lies D, Hernandez M, Kappler A, Mielke R, Gralnick J, Newman D (2005) *Shewanella oneidensis* MR-1 uses overlapping pathways for iron reduction at a distance and by direct contact under conditions relevant for biofilms. *Applied and Environmental Microbiology* **71**, 4414–4426.

Liger E, Charlet L, Van Cappellen P (1999) Surface catalysis of uranium(VI) reduction by iron(II). *Geochimica et Cosmochimica Acta* **63**, 2939–2955.

Lovley DR, Holmes DE, Nevin K (2004) Dissimilatory Fe(III) and Mn(IV) reduction. *Advances in Microbial Physiology* **49**, 219–286.

Ludwig KR (1991) *ISOPLOT: A Plotting and Regression Program for Radiogenic-Isotope Data*, Version 2.53. US Geological Survey, Reston, VA.

Matthews A, Morgans-Bell H, Emmanuel S, Jenkyns H, Erel Y, Halicz L (2004) Controls on iron-isotope fractionation in organic-rich sediments (Kimmeridge Clay, Upper Jurassic, southern England). *Geochimica et Cosmochimica Acta* **68**, 3107–3123.

Nevin K, Lovley D (2000) Lack of production of electron-shuttling compounds or solubilization of Fe(III) during reduction of insoluble Fe(III) oxide by *Geobacter metallireducens*. *Applied and Environmental Microbiology* **66**, 2248–2251.

Nevin K, Lovley D (2002) Mechanisms for Fe(III) oxide reduction in sedimentary environments. *Geomicrobiology Journal* **19**, 141–159.

Pecher K, Haderlein S, Schwarzenbach R (2002) Reduction of polyhalogenated methanes by surface-bound Fe(II) in aqueous suspensions of iron oxides. *Environmental Science and Technology* **36**, 1734–1741.

Pedersen H, Postma D, Jakobsen R, Larsen O (2005) Fast transformation of iron oxyhydroxides by the catalytic action of aqueous Fe(II). *Geochimica et Cosmochimica Acta* **69**, 3967–3977.

Reguera G, McCarthy K, Mehta T, Nicoll J, Tuominen M, Lovley D (2005) Extracellular electron transfer via microbial nanowires. *Nature* **435**, 1098–1101.

Roden EE (2006) Geochemical and microbiological controls on dissimilatory iron reduction. *Comptes Rendus Geoscience* **338**, 456–467.

Roden E, Zachara J (1996) Microbial reduction of crystalline iron(III) oxides: Influence of oxide surface area and potential for cell growth. *Environmental Science & Technology* **30**, 1618–1628.

Rosso K, Smith D, Dupuis M (2003a) An *ab initio* model of electron transport in hematite (alpha-Fe2O3) basal planes. *Journal of Chemical Physics* **118**, 6455–6466.

Rosso K, Zachara J, Fredrickson J, Gorby Y, Smith S (2003b) Nonlocal bacterial electron transfer to hematite surfaces. *Geochimica et Cosmochimica Acta* **67**, 1081–1087.

Schwertmann U, Cornell RM (1991) *Iron Oxides in the Laboratory*. Weinheim, New York.

Severmann S, Johnson C, Beard B, McManus J (2006) The effect of early diagenesis on the Fe isotope compositions of porewaters and authigenic minerals in continental margin sediments. *Geochimica et Cosmochimica Acta* **70**, 2006–2022.

Sherman D (1987) Molecular orbital (SCF-X-ALPHA-SW) theory of metal-metal charge transfer processes in minerals 1. Application to Fe^{2+} to Fe^{3+} charge transfer and 'electron delocalization' in mixed-valence iron oxides and silicates. *Physics and Chemistry of Minerals* **14**, 355–363.

Silvester E, Charlet L, Tournassat C, Gehin A, Greneche J, Liger E (2005) Redox potential measurements and Mossbauer spectrometry of Fe-II adsorbed onto Fe-III (oxyhydr) oxides. *Geochimica et Cosmochimica Acta* **69**, 4801–4815.

Skulan J, Beard B, Johnson C (2002) Kinetic and equilibrium Fe isotope fractionation between aqueous Fe(III) and hematite. *Geochimica et Cosmochimica Acta* **66**, 2995–3015.

Staubwasser M, von Blanckenburg F, Schoenberg R (2006) Iron isotopes in the early marine diagenetic iron cycle. *Geology* **34**, 629–632.

Stookey L (1970) Ferrozine: a new spectrophotometric reagent for iron. *Analytical Chemistry* **42**, 779–781.

Strathmann T, Stone A (2003) Mineral surface catalysis of reactions between Fe-II and oxime carbamate pesticides. *Geochimica et Cosmochimica Acta* **67**, 2775–2791.

Thamdrup B (2000) Bacterial manganese and iron reduction in aquatic sediments. *Advances in Microbial Ecology* **16**, 41–84.

Tronc E, Belleville P, Jolivet J, Livage J (1992) Transformation of ferric hydroxide into spinel by Fe(II) adsorption. *Langmuir* **8**, 313–319.

Tronc E, Jolivet J, Lefebvre J, Massart R (1984) Ion adsorption and electron-transfer in spinel-like iron oxide colloids. *Journal of the Chemical Society-Faraday Transactions I* **80**, 2619–2629.

Vargas M, Kashefi K, Blunt-Harris E, Lovley D (1998) Microbiological evidence for Fe(III) reduction on early Earth. *Nature* **395**, 65–67.

Welch S, Beard B, Johnson C, Braterman P (2003) Kinetic and equilibrium Fe isotope fractionation between aqueous Fe(II) and Fe(III). *Geochimica et Cosmochimica Acta* **67**, 4231–4250.

Wiesli R, Beard B, Johnson C (2004) Experimental determination of Fe isotope fractionation between aqueous Fe(II), siderite and 'green rust' in abiotic systems. *Chemical Geology* **211**, 343–362.

Williams A, Gregory K, Parkin G, Scherer M (2005) Hexahydro-1,3,5-trinitro-1,3,5-triazine transformation by biologically reduced ferrihydrite: Evolution of Fe mineralogy, surface area, and reaction rates. *Environmental Science and Technology* **39**, 5183–5189.

Williams A, Scherer M (2004) Spectroscopic evidence for Fe(II)-Fe(III) electron transfer at the iron oxide–water interface. *Environmental Science and Technology* **38**, 4782–4790.

Yamaguchi K, Johnson C, Beard B, Ohmoto H (2005) Biogeochemical cycling of iron in the Archean-Paleoproterozoic Earth: constraints from iron isotope variations in sedimentary rocks from the Kaapvaal and Pilbara Cratons. *Chemical Geology* **218**, 135–169.